

# Effect of Dust Deflagrations on Human Skin

A Major Qualifying Project submitted completed in partial fulfillment of  
the Bachelor of Science degree at

Worcester Polytechnic Institute, Worcester, MA

Submitted to:

Professor Ali S. Rangwala (Advisor)

Professor Nikolaos K. Kazantzis (Co-advisor)

James M. Grimard

Kevin Potter

With Acknowledgements to Xanxuan Xie and Daniel Karol

March 5, 2011



---

Advisor Signature



---

Co-advisor Signature

## **Abstract**

The aim of the study is to determine the damage done to human skin by a dust explosion in comparison to a gas explosion. This is achieved by using two different experimental methods, the steady state pre-heat and the flame velocity technique. In both of the experiments for a gas flame, the temperatures were determined for four different equivalence ratios. In the experiment for a dust flame, the temperatures were determined for one equivalence ratio. Results for the dust and gas flames are in good agreement for radiation and convection heat transfer. In addition, the factors that influence the heat flux from a dust flame are analyzed.

# Table of Contents

Abstract .....	2
Table of Figures .....	5
Table of Tables .....	6
1.0 Introduction .....	7
1.1 What Is a Dust Explosion? .....	7
1.2 Burn Types.....	9
1.3 Human Skin .....	9
2.0 Methodology.....	13
2.1 Theoretical Approach.....	13
2.2 Experimental Approach .....	18
3.0 Experimental Results.....	24
3.1 Steady-State Preheating .....	24
3.2 Gas and Dust Bunsen Burner Velocity Testing.....	26
4.0 Analysis .....	30
4.1 Steady-State Preheating .....	30
4.2 Gas Velocity.....	30
4.3 Measurement Error .....	31
4.4 Stationary and Moving Flame .....	31
4.5 Dust and Gas Flame .....	31
5.0 Conclusions .....	32
6.0 Recommendations .....	33
References .....	35
Appendix .....	37
Appendix A: Skin Density Calculation .....	37
Appendix B: Table of Values .....	38
Appendix C: Temperature of the Basal Layers with fluxes $q_1$ , $q_2$ , and $q_3$ .....	39
Appendix D: Critical Distance at which Pain is Felt.....	40
Appendix E: Preheat Temperature .....	42
Appendix F: Exposure Time versus Flame Thickness .....	50
Appendix G: Temperature of the Basal Layer Updated with the Preheat Temperature, Flux from Inside a Flame, and Velocity .....	52

Appendix H: Flux Required for Skin Damage and Skin Death .....	55
Appendix I: Servo Motor Velocity .....	56
Appendix J: Correction Factor .....	57
Appendix K: Equivalence Ratio Setup .....	60
Appendix L: Gas Equivalence Ratio 1 Raw Data .....	61
Appendix M: Gas Equivalence Ratio 1 Corrected .....	63
Appendix N: Gas Equivalence Ratio Raw Data .....	66
Appendix N: Gas Equivalence Ratio 2 Corrected .....	68
Appendix O: Gas Equivalence Ratio 3 Raw Data .....	71
Appendix P: Gas Equivalence Ratio 3 Corrected .....	73
Appendix Q: Gas Equivalence Ratio 4 Raw Data .....	76
Appendix R: Gas Equivalence Ratio 4 Corrected .....	78
Appendix S: Dust Equivalence Ratio Raw Data .....	81
Appendix T: Dust Equivalence Ratio Corrected .....	83
Appendix U: Theoretical Critical Distance .....	85

## Table of Figures

Figure 1: Dust Explosion Pentagon .....	7
Figure 2: Layers of Human Skin and Thermal Resistances, $k$ represents thermal conductivity, $x_b$ represents depth of epidermis, $L$ represents depth of dermis and hypodermis, and $R$ represents thermal resistance .....	10
Figure 3: Temperature of the Basal Layer ( $T_b$ ) [ $^{\circ}\text{C}$ ] when exposed to Constant Heat Flux ( $q''$ ) [ $\text{kW}/\text{m}^2$ ] ...	12
Figure 4: Flux [ $\text{W}/\text{m}^2$ ] required for the Temperature of the Basal Layer to Reach $44^{\circ}\text{C}$ .....	13
Figure 5: Flux required for the Temperature of the Basal Layer to Reach $72^{\circ}\text{C}$ .....	14
Figure 6: View Factor Geometry .....	14
Figure 7: Servo Motor Apparatus.....	18
Figure 8: Gas Flame with Cone and Diffusive Sections Outlined .....	20
Figure 9: Steady State Test for a Dust Flame with a concentration of $44\text{g}/\text{min}$ of Coal Dust of sizes ( $60\text{-}95\ \mu\text{m}$ ) .....	21
Figure 10: Thermocouple Passing through Cone of Flame .....	22
Figure 11: Sample Picture of the Dust Flame without a visible Cone.....	23
Figure 12: Gas Flame Preheat Temperature vs. Distance for an Equivalence Ratio of 1.00 .....	25
Figure 13: Dust Flame Preheat Temperature vs. Distance for an Equivalence Ratio of 1.67 .....	26
Figure 14: Gas Flame Velocity vs Temperature for an Equivalence Ratio of 1.00 .....	27
Figure 15: Gas Flame Velocity vs Temperature for an Equivalence Ratio of 0.78 .....	28
Figure 16: Gas Flame Velocity vs Temperature for an Equivalence Ratio of 1.16 .....	28
Figure 17: Gas Flame Velocity vs Temperature for an Equivalence Ratio of 1.37 .....	29
Figure 18: Gas Flame Preheat Temperature vs. Distance for an Equivalence Ratio of 0.78 .....	70
Figure 19: Gas Flame Preheat Temperature vs. Distance for an Equivalence Ratio of 1.16 .....	75
Figure 20: Gas Flame Preheat Temperature vs. Distance for an Equivalence Ratio of 1.37 .....	80

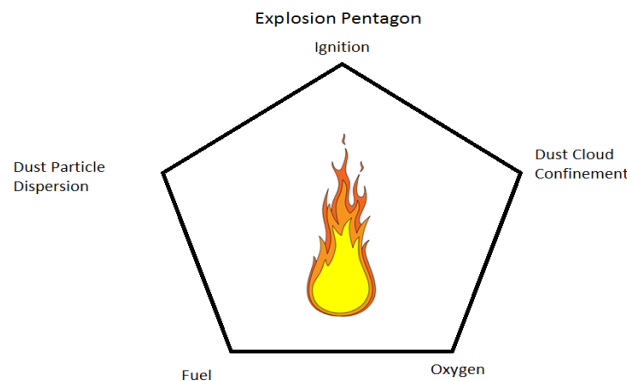
## Table of Tables

Table 1: Pre-heating temperature of the basal layer for varying flame velocities .....	16
Table 2: Steady State Distances for Gas Equivalence Ratio 3 ( $\phi=1.16$ ) .....	21
Table 3: Values Used to Calculate Basal Layer Temperature.....	38
Table 4: Basal Layer Temperature Calculated for 60 Seconds.....	39

# 1.0 Introduction

## 1.1 What Is a Dust Explosion?

A dust explosion is the fast combustion of dust particles suspended in the air in an enclosed location. Dust explosions can occur where any powdered combustible material is present in an enclosed atmosphere (i.e. sugar factories, coal mines) [6]. A dust explosion requires five elements as shown in Figure 1:



**Figure 1: Dust Explosion Pentagon**

The first element required is combustible dust. A combustible dust is a type of atmospheric hazard that consists of fine grains of material that are capable of exploding or catching fire [3]. Additionally, “any particle that has a surface area to volume ratio greater than that of a 420  $\mu\text{m}$  diameter sphere should also be deemed a combustible dust” [4]. The material needs to be an oxidizer, an explosive, or a pyrophoric material [2]. The second element needed is an ignition source of sufficient energy denoted by the minimum ignition energy (MIE) or minimum dust cloud ignition temperature (auto-ignition temperature). The MIE determines the smallest amount of electrostatic spark energy that is required to initiate a dust cloud explosion. The auto-ignition temperature is the lowest temperature at which it will spontaneously ignite in a normal atmosphere without an external source of ignition, such as a flame or spark. The third element is oxygen which plays a significant role in the hazard associated with

combustible dust. For example, if the oxygen levels are around 24% (an increase of just 3% from the ambient oxygen concentration) the combustion velocity doubles. In comparison to the Fire Triangle, dust explosions require two additional elements: confinement and dispersion [5]. However, the dust cloud does not only need to be dispersed in the air, it also needs to have a sufficient concentration of dust in the cloud. A dust cloud has two boundaries, a lower explosion limit (LEL) and an upper explosion limit (UEL), and for an explosion to occur the concentration of dust needs to be in between these limits. Typical concentrations are 60 (g/m<sup>3</sup>) for sugar, bituminous coal, milk powder, and fructose [24].

### ***1.1.1 Dust Explosion Case Studies***

To fully understand the capabilities of dust explosions, one must examine the damage done by a dust explosion from several case studies. Each case study describes the incident leading to the explosion, the average age of the injured, and the classification of burns suffered. The first case study observed dealt with a sawdust explosion. A fire had not been fully extinguished in a storage silo and resulted in the injury of a worker, a healthy, 33-year old male. He suffered burns to 33% of his body; 15% of said burns were full thickness burns (3<sup>rd</sup> degree burns) [14]. The second case examined many different types of burns (e.g. electrical, explosion, hot oil, and hot water) and the type of damage that they cause to the skin. Four people, averaging 35 years old, were injured. They suffered burn injuries on approximately 33% of their body. Of that 33%, 18% of the burns were 3<sup>rd</sup> degree. In 75% of the cases studied, soot residues were prominent [13]. Over a 13- year period, the final case study examined 339 patients burned in gun powder explosions. The patients averaged 37 years old. 41% of the patients' bodies had burns, and 21.7% of their bodies were affected by 3<sup>rd</sup> degree burns. The total burn area ranged between 1% and 98% and had a mean of 40.9%. The full thickness burns, or 3<sup>rd</sup> degree burns, ranged from 0-96% and had a mean of 21.7%. The most injured areas on the patients were the head, neck, and upper limbs [12]. Although these case studies look at different cases, they show correlations in their data about the damage caused to the skin by dust explosions. On average, a person of 33 years



of age had been burned in the upper third of their body, and of those burns approximately 18% were 3<sup>rd</sup> degree burns.

## **1.2 Burn Types**

Thermal damage has been evaluated by three degrees: first, second, and third. In a first degree burn only the dermis is affected and is marked by redness in the affected areas. Next, A second degree burn is the complete destruction of the dermis and is broken into two types: superficial and deep. Superficial second degree burns have no damage done to the dermis while deep second degree burns have minor damage to the dermis. In both cases the skin is blistered and very pale white or has mottled colors under the blisters. Finally, a third degree burn is the complete necrosis (75% destruction or greater) of dermis which may include damage to subcutaneous fat [10].

## **1.3 Human Skin**

Human skin has three different regions as shown in Figure 2: (1) epidermis, (2) dermis, (3) hypodermis. Each layer provides different roles and is composed of sub-layers. The outermost layer of skin is the epidermis. Depending on the location on the human body, the thickness of the epidermis can vary. It ranges from a minimum thickness of 0.05 mm on the eyelids to a maximum thickness of 1.5 mm on the palms and soles [15]. The epidermis is comprised of five different sub-layers. The outermost sub-layer is the stratum corneum, which is composed of only non-living cells. The other sub-layers, in order of the outermost to innermost, are the stratum lucidum, stratum granulosum, stratum spinosum, and stratum malphigi. The cells that make up the stratum lucidum and stratum granulosum are in transition between dead and dying. This transition, which varies depending on the location of the skin, is one of the causes of the variations in skin thickness [10]. The stratum malphigi is composed of two more layers, the stratum basale and the stratum germinativum, and the latter aids in the body's heat regulation [10]. The next layer of skin is the dermis, which is composed of two layers: the papillary dermis (the upper layer) and the reticular dermis (the lower layer). Blood vessels, nerves, hair follicles,

and sweat glands are located in the dermis [16]. Mastocyte cells, which contain heparin and histamine, the cause of the red flush of a burn, are also found in the dermis. The final layer of skin is the hypodermis, also known as the subcutaneous fat tissue. This layer is composed mostly of fat which also explains the variation of skin thicknesses for different locations on the body for different genders. The hypodermis also includes blood vessels, nerves, hair follicle roots, and sheets of muscle in certain locations (i.e. the face, hand, and scalp). To simplify human skin, each of these three layers in Figure 2 represents a layer in human skin. In order to determine the temperature at the base of the hypodermis, the resistances of the three layers need to be calculated.

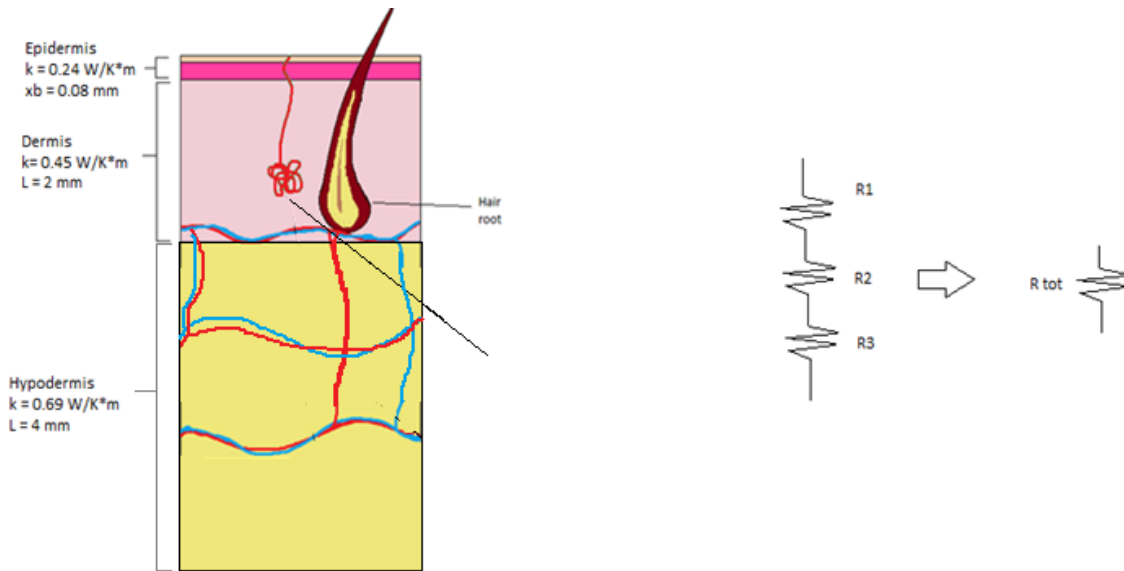


**Figure 2: Layers of Human Skin and Thermal Resistances, k represents thermal conductivity, xb represents depth of epidermis, L represents depth of dermis and hypodermis, and R represents thermal resistance**

Equation 1 shows how to calculate the thermal resistance for a single layer where L is the thickness (m), k is the thermal conductivity (W/K\*m), and A is the area (m<sup>2</sup>). Equation 2 depicts the calculation for total resistance from resistances in series [17].

$$R = L/kA \quad \mathbf{1}$$

$$R = R1 + R2 + R3 \quad \mathbf{2}$$

Equation 3 is a damage integral equation that can determine when 1<sup>st</sup>, 2<sup>nd</sup>, or 3<sup>rd</sup> degree burns will occur [10].

$$\Omega = \int_0^t P \exp\left(\frac{-\Delta E}{RT_b}\right) dt \quad 3$$

In Equation 3, P is the pre-exponential term,  $\Delta E$  is the activation energy,  $T_b$  is the temperature at the basal layer, and R is Boltzmann's constant. By being able to calculate what type of burn will occur based on these parameters, Equation 3 is able to determine the damage a dust explosion does to human skin. Upon integration of Equation 3, superficial second degree burns can be predicted "by calculating the time when  $\Omega = 1$  based on the temperature of the basal layer" and becomes Equation 4 [10].

By determining the final resistance, the epidermis, dermis, and hypodermis can be treated as a single entity. Equation 4 uses this principle to calculate the temperature of the basal layer and is a function of incident heat flux ( $\dot{q}''$ ), thermal conductivity ( $k$ ), thermal diffusivity ( $\alpha$ ), time (t), exposure time ( $\tau$ ), and basal layer depth ( $x_b$ ) [10]. The thermal diffusivity ( $\alpha$ ), can further be defined by the equation  $\alpha = \frac{k}{\rho * c}$  where k is the thermal conductivity,  $\rho$  is the density, and c is the specific heat.

$$T_b = T_0 + \frac{\dot{q}''}{k} \left[ \frac{2\sqrt{\alpha t}}{\sqrt{\pi}} \exp\left(-\frac{x_b^2}{4\alpha t}\right) - x_b \operatorname{erfc}\left(\frac{x_b}{2\sqrt{\alpha t}}\right) \right] - \frac{\dot{q}''}{k} \left[ \frac{2\sqrt{\alpha(t-(1.6\tau))}}{\sqrt{\pi}} \exp\left(-\frac{x_b^2}{4\alpha(t-(1.6\tau))}\right) - x_b \operatorname{erfc}\left(\frac{x_b}{2\sqrt{\alpha(t-(1.6\tau))}}\right) \right] \quad 4$$

Equation 4 can be solved since many of the units can be calculated or found by looking through literature. Values for the thermal conductivity, basal layer depth, and heat capacity were determined by consulting the literature. These values are shown in Table 1 in Appendix B. The value for the skin density at the basal layer was calculated to be 24,968 kg/m<sup>3</sup> as determined in Appendix A. By solving for different values of the incident heat flux ( $\dot{q}''$ ), the basal layer temperature can be compared by time as a function of the incident heat flux as shown in Figure 3.

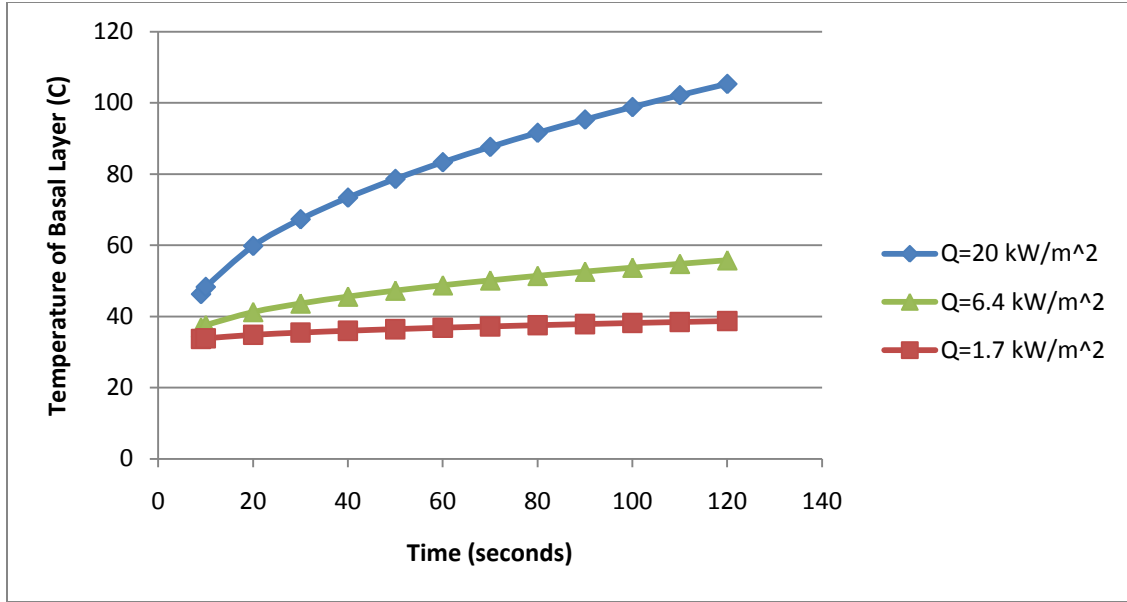


Figure 3: Temperature of the Basal Layer ( $T_b$ ) [ $^{\circ}\text{C}$ ] when exposed to Constant Heat Flux ( $q''$ ) [ $\text{kW}/\text{m}^2$ ]

By looking through heat transfer literature, Equation 4 was similar when compared with Equation 5 which illustrates a semi-infinite solid with a constant surface heat flux.

$$T(x, t) - T_i = \frac{2q_0''(\frac{\alpha t}{\pi})^{1/2}}{k} \exp\left(\frac{-x^2}{4\alpha t}\right) - \frac{q_0''x}{k} \operatorname{erfc}\left(\frac{x}{2\sqrt{\alpha t}}\right) \quad 5$$

Equation 5 has the same variables as Equation 4 with slight variations in nomenclature. The following terms from Equations 4 and 5 are analogous to each other:  $q_0'' = \dot{q}''$ ,  $T_i = T_0$ ,  $T(x, t) = T_b$ , and  $x = x_b$ . The remaining variables have identical nomenclature (e.g. thermal conductivity, thermal diffusivity, and time) [22].

## 2.0 Methodology

### 2.1 Theoretical Approach

#### 2.1.1 Burn Threshold

The human skin, while well suited for moderate temperatures, cannot handle extreme heating. Damage to the skin begins once the temperature of the base layer of the dermis (the basal layer) exceeds 44°C. This temperature is the lower burn threshold for human skin, where 1<sup>st</sup> degree burns begin to occur. As the temperature of the basal layer increases, the damage to the skin and the severity of the burn increases as well. The upper burn threshold temperature for human skin is 72°C. At this temperature, the skin is destroyed instantaneously.

By solving Equation 4 for 44 and 72°C, the heat flux that causes the skin to reach 44 and 72°C at a given time can be calculated, and is shown in Figures 4 & 5.

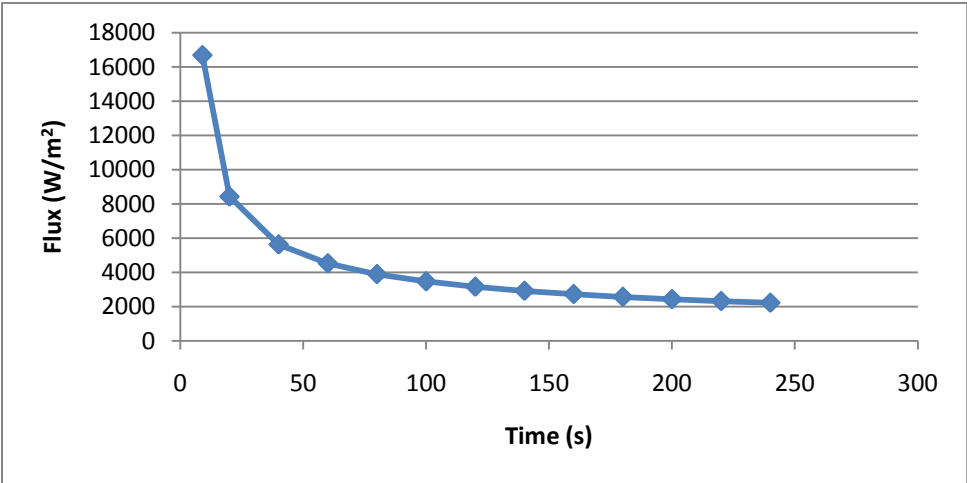


Figure 4: Flux [W/m<sup>2</sup>] required for the Temperature of the Basal Layer to Reach 44°C

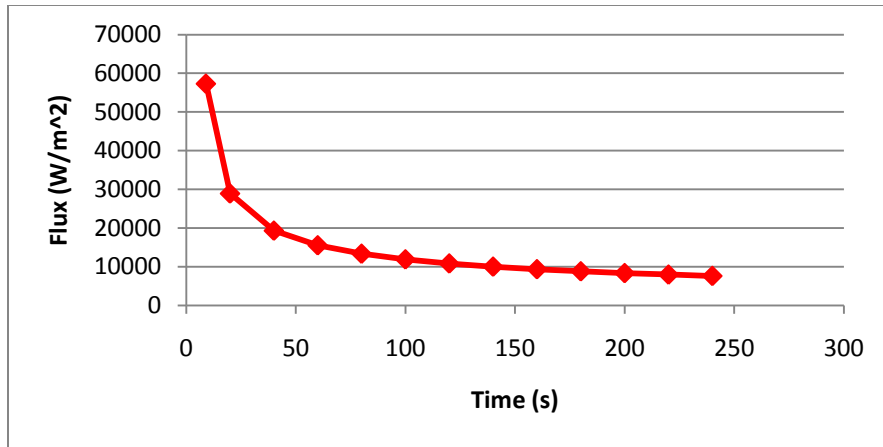


Figure 5: Flux required for the Temperature of the Basal Layer to Reach 72°C

### 2.1.2 Heat Flux

In order to quantify the damage a dust explosion does to the human skin, a mathematical model was developed using Equation 4, in which the heat flux was determined and the equation was solved for the basal layer temperature. The heat flux was determined by using a view factor, which is the proportion of radiation that leaves one surface and strikes another. The view factor is described in Equation 6 in which a planar element,  $dA_1$ , lies in a plane parallel to a square,  $A_2$ , and passes through the center of the square. Its geometry is shown in Figure 6 where  $dA_1$  refers to skin and  $A_2$  refers to the high temperature combustion wave.

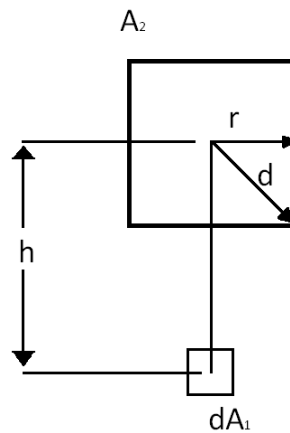


Figure 6: View Factor Geometry

$$F_{d1-2} = \frac{nD}{\pi(1+D^2)^{1/2}} \tan^{-1} \left[ \left( \frac{R^2 - D^2}{1+D^2} \right) \right] \quad 6$$

In Equation 6,  $D = \frac{d}{h}$  and  $R = \frac{r}{h}$  where  $d$  is the diameter of the polygon,  $r$  is the radius,  $h$  is the distance between element  $A_2$  and  $dA_1$ , and  $n$  is the number of sides of the square (i.e. four). Once the view factor was determined, the heat flux was calculated using Equation 7, where  $F$  is the view factor,  $\epsilon$  is the emissivity,  $\sigma$  is the Stefan-Boltzmann constant ( $W/m^2K^4$ ), and  $T$  is the temperature (K).

$$Q = F\epsilon\sigma T^4 \quad 7$$

It is important to note that the aforementioned heat flux is the heat flux before the flame reaches the skin. The heat flux when the flame touches the skin is described by Equation 8, where  $\sigma$  is the Stefan-Boltzmann constant ( $W/m^2K^4$ ), and  $T$  is the temperature (K). Equation 8 assumes that the emissivity of skin is equal to one (1).

$$Q = \sigma T^4 \quad 8$$

To determine the damage done to the skin, two different profiles were studied. The pre-heating profile is the time from when the pain is felt from the flame, at approximately  $1.7 \text{ kW/m}^2$ , to when the flame is nearly in direct contact with the skin. The heat flux for the pre-heating profile is calculated from Equation 7. The second profile is the time from when the flame directly touches the skin until it dissipates. The heat flux for this profile is calculated from Equation 8. For plotting the results, it was assumed that the flame travels a distance of 1m before it reaches the skin as shown in Appendix D.

### **2.1.3 Pre-Heating**

The first type of heat exposure is when the skin is preheating. The amount which the skin preheats varies with the flame velocity and the flame temperature. As the velocity of the flame increases, the amount of heat transfer decreases. An example of this is when a flame traveling at 1 m/s heats the skin from  $32.5^\circ\text{C}$  to  $53.3^\circ\text{C}$ . However when a flame travels at 10 m/s, the heat transfer is 10

times smaller. At 10 m/s the temperature of the basal layer only increases to 35.5°C from 32.5 °C. This is further discussed in Appendix E. Additionally, the temperature of the flame is directly proportional to the heat flux as shown previously in Equation 7. If the temperature was doubled, the heat flux would increase by a factor of 16.

In order to determine the pre-heating temperatures, the distance at which pain is felt from the flame was determined for the given flame velocity of 1 m/s. The distance at which pain was felt was determined to be 0.6445 meters from the skin. Multiple iterations were then done between that distance and 0.0184 meters, the distance at which the skin was considered in direct contact with the flame. Next, the iterations were then modified to factor in the effects of different velocities as shown in Appendix G. The averages of the exposure time, heat flux,  $q/k_h$ , and  $q/k_c$ , as shown in Table 1, were used to determine the temperature of the basal layer during the pre-heating profile.

**Table 1: Pre-heating temperature of the basal layer for varying flame velocities**

Velocity (m/s)	Time (s)	Exposure Time ( $\tau$ )	Heat Flux ( $W/m^2$ )	$q/k_h$	$q/k_c$	Temperature of the Basal Layer (°C)
1	0.98	0.0179	46,427.82	78,985.75	102,761.88	53.3
3	0.33	0.00596	15,475.94	26,328.58	34,253.96	39.5
5	0.20	0.00358	9,285.56	15,797.15	20,552.38	38.4
10	0.19	0.00179	4,642.78	7,898.57	10,276.19	35.5

### **2.1.4 Direct Flame Contact**

The second type of heating is from direct contact of the skin with the flame. When the skin is in direct contact with the flame, the basal layer temperature is affected by the variation in flame velocity, flame temperature, and flame thickness. Equation 8 shows that, when the skin is directly in the flame, heat transfer is no longer affected by the view factor or the emissivity and is solely dependent upon the flame temperature. As shown in Appendix G, heat flux increases significantly without the view factor.



The flame thickness for a dust explosion varies between 1mm and 10cm and needs to pass through roughly 2mm of skin to reach the basal layer. The total thickness (flame thickness and skin thickness combined) divided by the velocity equals the time it takes for the flame to reach the basal layer as shown in Appendix F. The flame thickness affects the temperature of the basal layer, because as the thickness increases, the skin is exposed to the flame for a longer amount of time which increases the basal layer temperature.

Because Equation 4 is solved for an average skin temperature, it has to be modified to include the following: the preheat temperatures, flame thickness, the time required to preheat the skin, and the exposure time for different flame thicknesses. Furthermore, multiple iterations needed to be calculated in order to determine the change in the temperature of the basal layer for the various velocities. These iterations are shown in Appendix G.

## 2.2 Experimental Approach

### 2.2.1 Servo Motor Apparatus

In order to simulate a dust explosion, a 40 gauge Type-K thermocouple (0.0799 mm) with a ceramic cylindrical shell (circled in blue) was attached to the rotating arm of the servo motor apparatus (SMA), created and programmed by Daniel Karol, to pass through the cone of a flame at ten different velocities ranging from 0.05 to 1.16 m/s as shown in Figure 7. The velocity range was chosen based on characteristic velocities found in typical dust deflagrations. The SMA was equipped with a button (circled in red) and a potentiometer (circled in green) to activate the apparatus and adjust the velocity of the apparatus respectively.

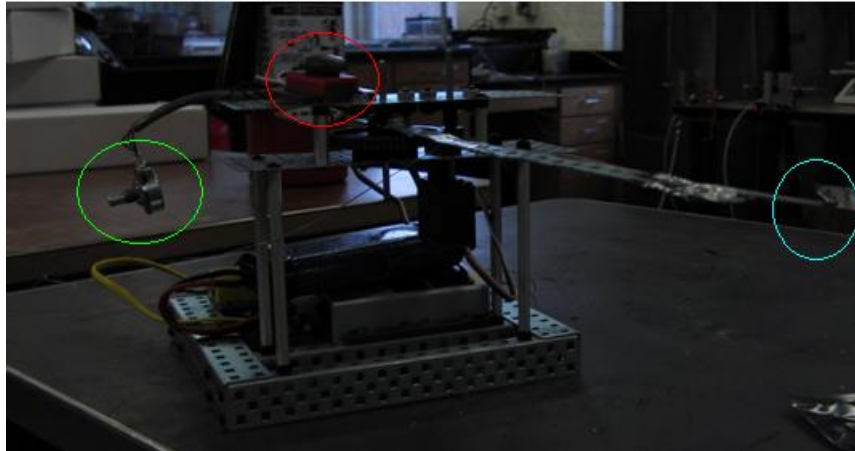


Figure 7: Servo Motor Apparatus

The SMA apparatus was chosen due to the multiple advantages it has for this experiment. In order to determine the damage of a dust deflagration to the human skin, there needed to be some aspect of the experiment that moved at a constant velocity. The two options were either a stationary thermocouple and a moving flame, or a moving thermocouple and a stationary flame. With the latter option, there would not be any danger from a moving flame. Also, the SMA apparatus could be run at a constant velocity and provide reliable, repeatable results. Thus, for these reasons, the SMA apparatus was chosen for the experiment.

The SMA apparatus is composed of a metal body and a rotating arm. The microcontroller, the gray box in Figure 7, is the interface for the servo motor. In the microcontroller, there are ports for the servo motor, the programming hardware, potentiometer, and a battery for a power source. The programming hardware, which is composed of a USB to serial cable, programming module, and RJ14 6-pin cable, sends information between the microcontroller and a computer. Using a computer program, the velocity from the potentiometer as well as any adjustments made to the potentiometer can be obtained.

To find ten velocities, the arc length and the time to pass along the arc length was required. As shown in Appendix I, the angle of movement for the SMA was  $50^\circ$  with an arm length of 33.7 cm which meant that the total distance traveled by the arm was 29.4 cm. The SMA had several time stamps (in ms) already programmed into the device. Using the previous information we were able to attain ten velocities as shown in Appendix I.

### ***2.2.2 Equivalence Ratio***

In order to determine four equivalence ratios, the stoichiometric volumetric flow rates were calculated first. These were determined by that laminar burning velocity of methane (30 to 50 cm/s). In order for the flame to stay steady, these values needed to be two to five times greater which changed our values to 60 to 250 cm/s. Additionally for a 1 cm flame, meaning the nozzle diameter is 1 cm, the area of the flame is  $0.785 \text{ cm}^2$ . Multiplying these values together and by a correction factor of 1.2 gives a volumetric flow rate of 56.55 cc/s to 235.62 cc/s. By dividing by the densities of air and natural gas, the masses of air and natural gases we found as shown in Appendix K. The air fuel ratio was then calculated by dividing the mass of air by the mass of the natural gas. In order to have a premixed natural gas flame, the fuel needed to stay within its flammability limit of approximately 4-17%. Four percentages were chosen between the upper and lower limits (10.0%, 12.5%, 8.8% and 7.5%) to attain four air fuel (AFRs) ratios (17.2, 13.4, 19.9, and 23.6 respectively). These AFRs were then divided by the

stoichiometric AFR to attain the four equivalence ratios:  $\phi=1.00$ , 0.78, 1.16, and 1.37 respectively. Figure 8 shows a gas flame for  $\phi=1.00$  where the cone and diffusive part of the flame has been outlined.

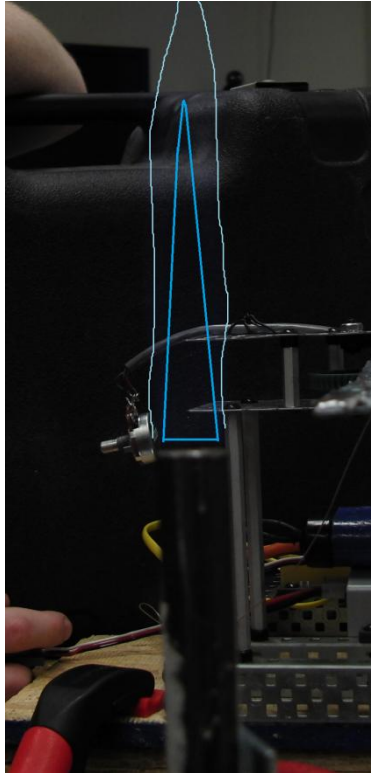


Figure 8: Gas Flame with Cone and Diffusive Sections Outlined

### ***2.2.3 Steady-State Testing***

To simulate the effect of skin preheating, temperature measurements were taken at set distances based off of the critical distance. In this case, the critical distance is the distance at which the temperature from the thermocouple increases above ambient temperature. Using a regular ruler, distances of half inches were marked on a flat aluminum bar. The aluminum ruler was then clamped to a ring stand and leveled off using a level, and the end of ruler was then placed on the edge of burner nozzle. The distances tested for both the dust and gas tests are the same. An example of the preheat distances and temperatures from gas equivalence ratio three (GER3) are shown in Table 2. Figure 9 shows the setup of the steady state testing.

Table 2: Steady State Distances for Gas Equivalence Ratio 3 ( $\phi=1.16$ )

Preheat				
Distance (cm)	Trial 1 (C)	Trial 2 (C)	Trial 3 (C)	Trial 4 (C)
19.05	24.50	24.83	25.56	25.56
16.51	24.61	25.50	27.28	25.83
13.97	24.94	25.67	29.44	26.67
11.43	26.67	28.00	29.61	28.94
8.89	28.67	28.17	29.11	30.83
6.35	29.50	29.11	31.44	31.61
3.81	31.89	31.06	33.50	34.89
1.27	50.94	50.06	54.72	57.11
0.635	114.67	146.39	201.83	130.50
0	933.33	1129.44	857.22	1244.44

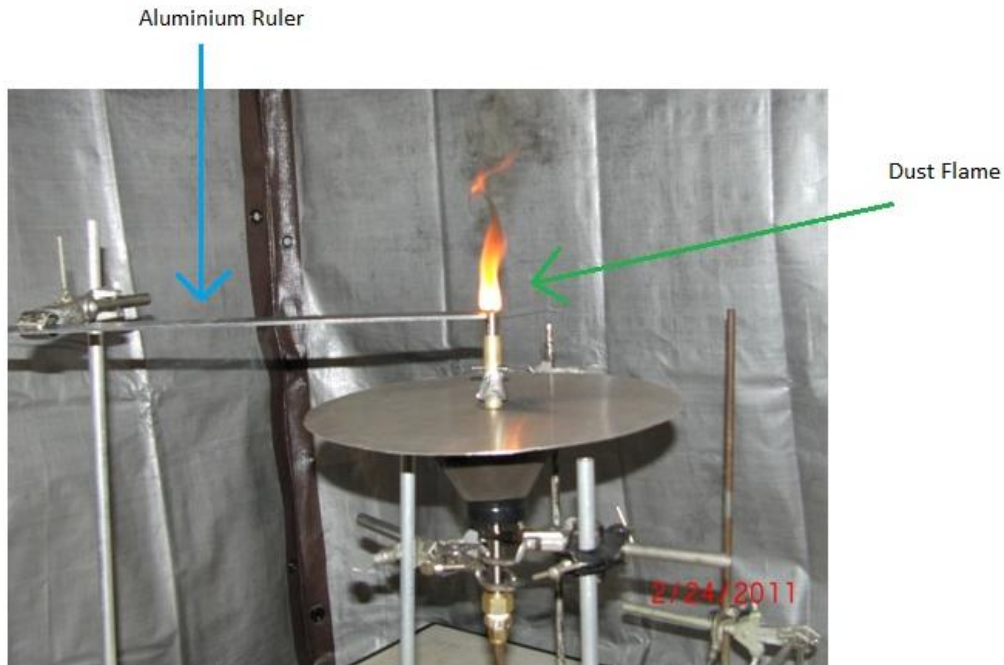
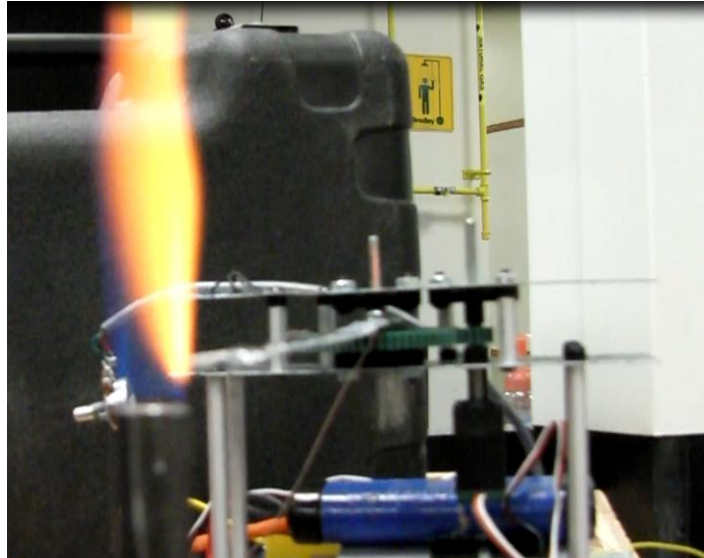


Figure 9: Steady State Test for a Dust Flame with a concentration of 44g/min of Coal Dust of sizes (60-95  $\mu\text{m}$ )

#### 2.2.4 Gas and Dust Bunsen Burner Velocity Testing

The SMA was set up so that the thermocouple would pass through the center of cone of the flame as shown in Figure 10.



**Figure 10: Thermocouple Passing through Cone of Flame**

After each trial for the ten velocity tests, the SMA arm was stabilized and the test was done an additional three times. The sequences of tests were then completed for an additional three equivalence ratios ( $\phi=0.78, 1.16, 1.37$ ). In order to attain the temperatures for each run the thermocouple was attached to a data acquisition system NI. Insta Cal<sup>®</sup> was then able to then output the values into Microsoft Excel<sup>®</sup>. The same procedure was done for the dust tests. However, only one equivalence ratio data set was able to be completed. As shown in Figure 11, there is no visible cone of which to collect data from; thus the diffusion flame one inch above the burner nozzle was measured instead of the cone of the flame. The port width of the apparatus is 0.635cm. The dust used was Pittsburgh seam bituminous coal with particle sizes between 75-90  $\mu\text{m}$ . The apparatus used was as described in "Study of Interaction of Entrained Coal Dust Particles in Lean Methane – Air Premixed Flames" [25]. For the dust test an equivalence ratio of 1.67 was used.

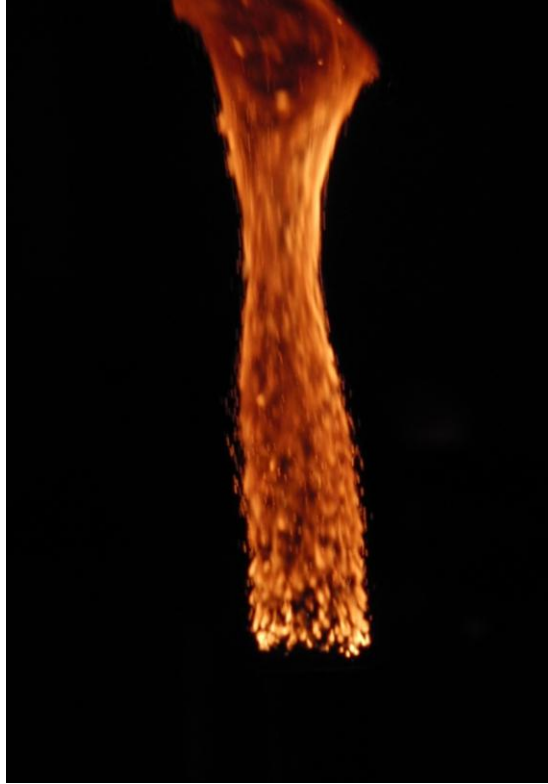


Figure 11: Sample Picture of the Dust Flame without a visible Cone

## 3.0 Experimental Results

### 3.1 Steady-State Preheating

For the steady-state, preheating section of the experimental procedure, five different equivalence ratios were tested. Four equivalence ratios were tested for the gas flame (1.00, 0.78, 1.16, 1.37), while one equivalence ratio was tested for the dust flame (1.67).

Figure 12 shows the temperature from the gas flame as a function of distance for an equivalence ratio of 1.00. As was expected, Figure 12 showed a rather constant temperature up until the thermocouple was directly next to the flame, in which the temperature increased dramatically. However, as the thermocouple was directly next to the flame, the temperatures varied greatly between the different trials. Because K-type thermocouples were used, they were approaching their upper limit for a temperature reading, which could have contributed to this noticeable difference in temperatures among the trials. The figures for the steady-state gas flame with the other three different equivalence ratios were nearly identical to Figure 12. As stated before, the only noticeable variation was the final data point that was directly next to the flame.



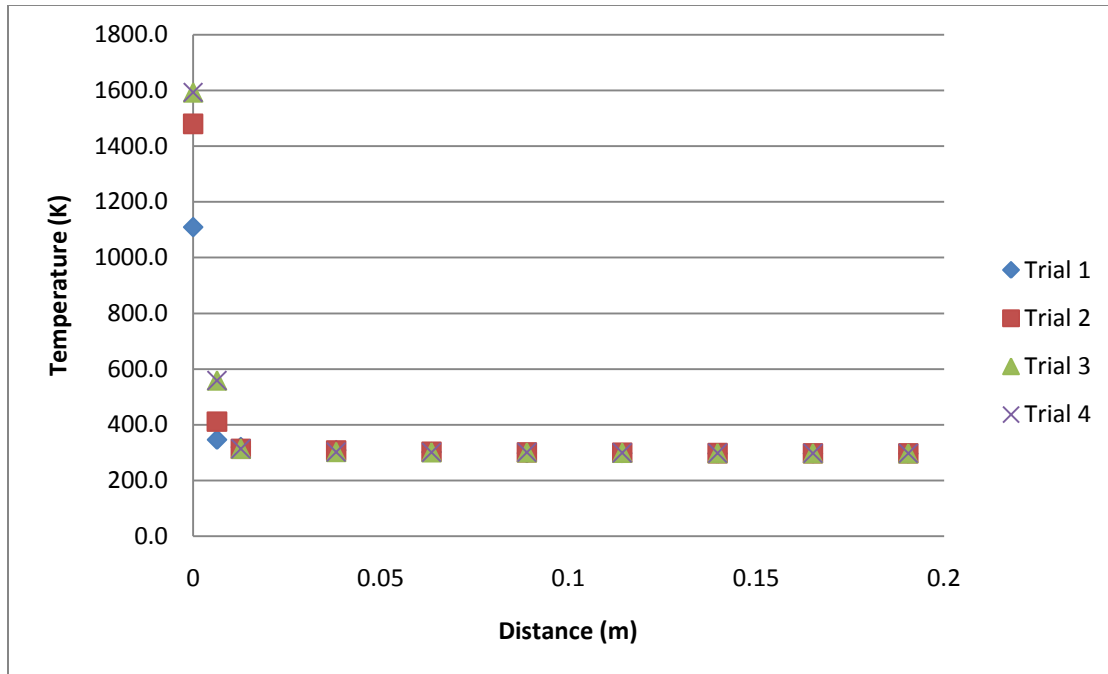


**Figure 12: Gas Flame Preheat Temperature vs. Distance for an Equivalence Ratio of 1.00**

Figure 13 shows the temperature from the dust flame as a function of distance for an equivalence ratio of 1.67. The trend, as expected, was similar to the gas flame experiment runs in which the temperature increased dramatically as the thermocouple was directly next to the flame. However, the temperature at this point was generally lower for the dust flame than for the gas flame. While the gas flame varied from 1100-1600 K, the dust flame temperature ranged from 1100-1200 K.

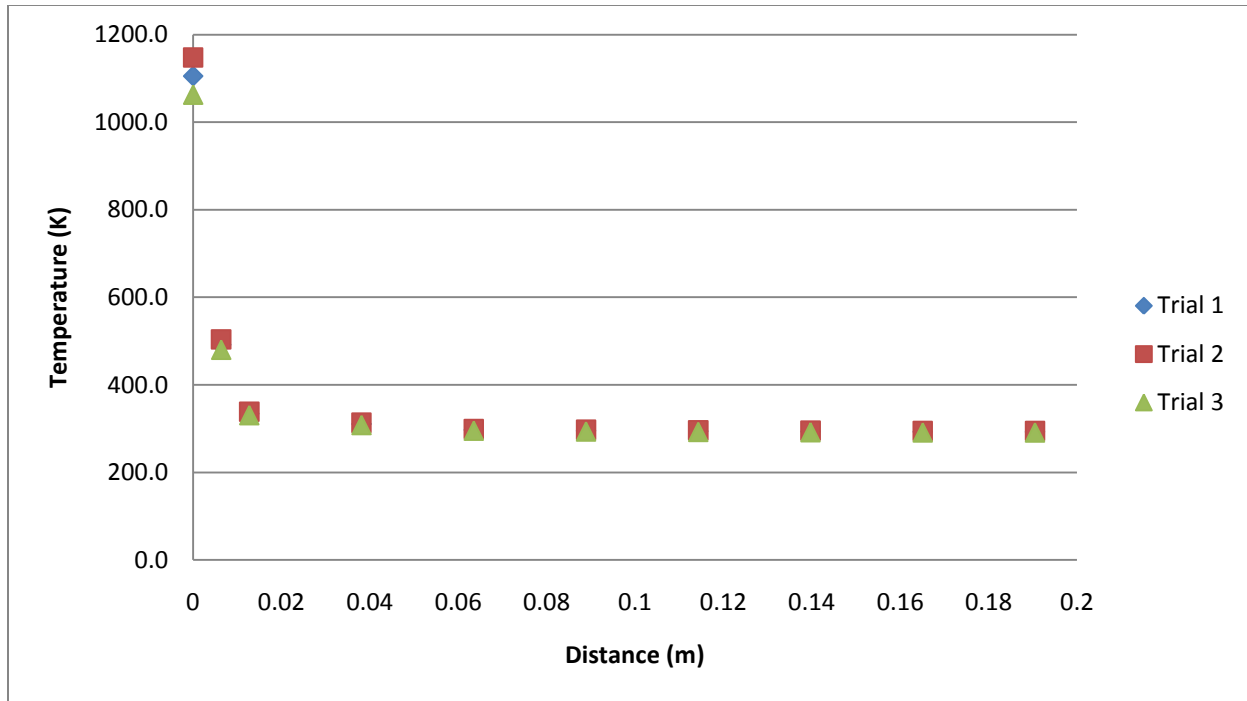
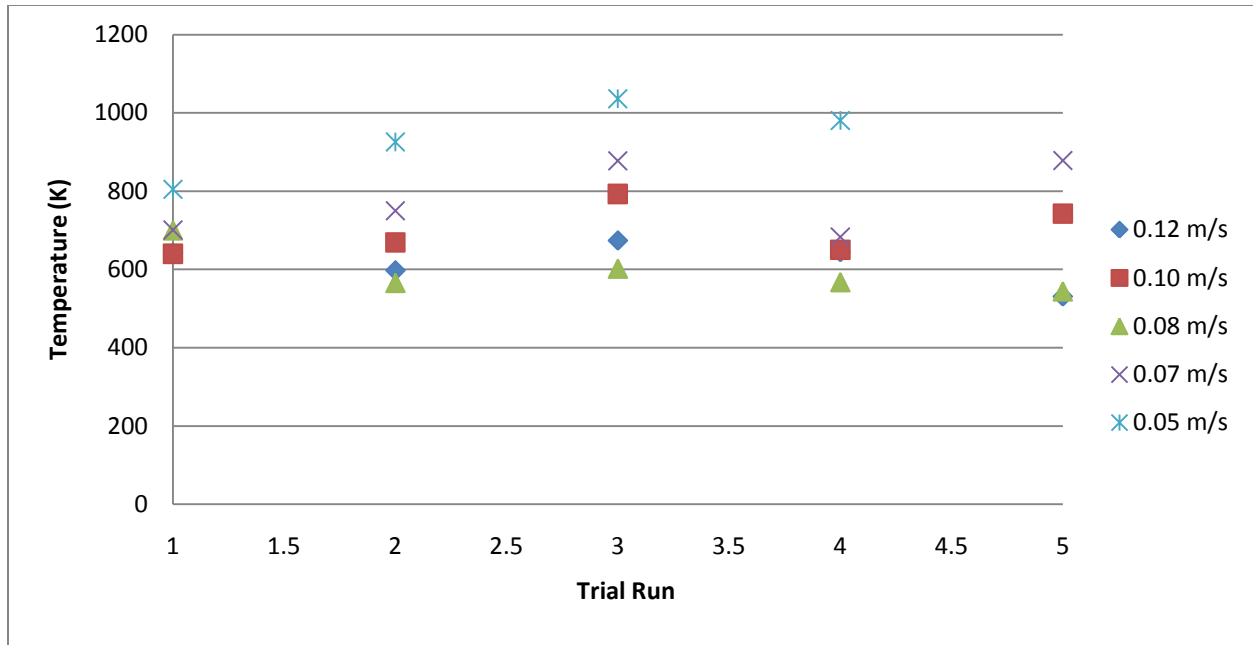


Figure 13: Dust Flame Preheat Temperature vs. Distance for an Equivalence Ratio of 1.67

### 3.2 Gas and Dust Bunsen Burner Velocity Testing

For the velocity experiments, the four equivalence ratios used for the steady-state preheating for the gas flame were used again. Initially, ten different velocities were tested; however, due to the limitations of the scanning rate for the equipment, the five fastest velocities could not be used due to the unreliability of the data obtained. The velocity range finally chosen was between 0.05 – 0.12 m/s.

Figure 14 shows the temperatures for the given velocities over a certain amount of trial runs and an equivalence ratio of 1.00. Although there were some variations, the general trend was that as the velocity decreased the temperature increased. This general trend agrees with the theoretical approach in Section 2.1.



**Figure 14: Gas Flame Velocity vs Temperature for an Equivalence Ratio of 1.00**

Figure 15 shows the temperatures for the given velocities over a certain amount of trial runs for an equivalence ratio of 0.78. The trend of an increasing temperature with decreasing velocity is observed in this figure as in the previous figure. While the temperatures in Figure 14 are in the same range as the previous figure, the average temperatures for the velocities are slightly lower. This is expected since the equivalence ratio isn't 1.00. When compared to the equivalence ratio of 1.00, any other equivalence ratio should have lower temperatures.

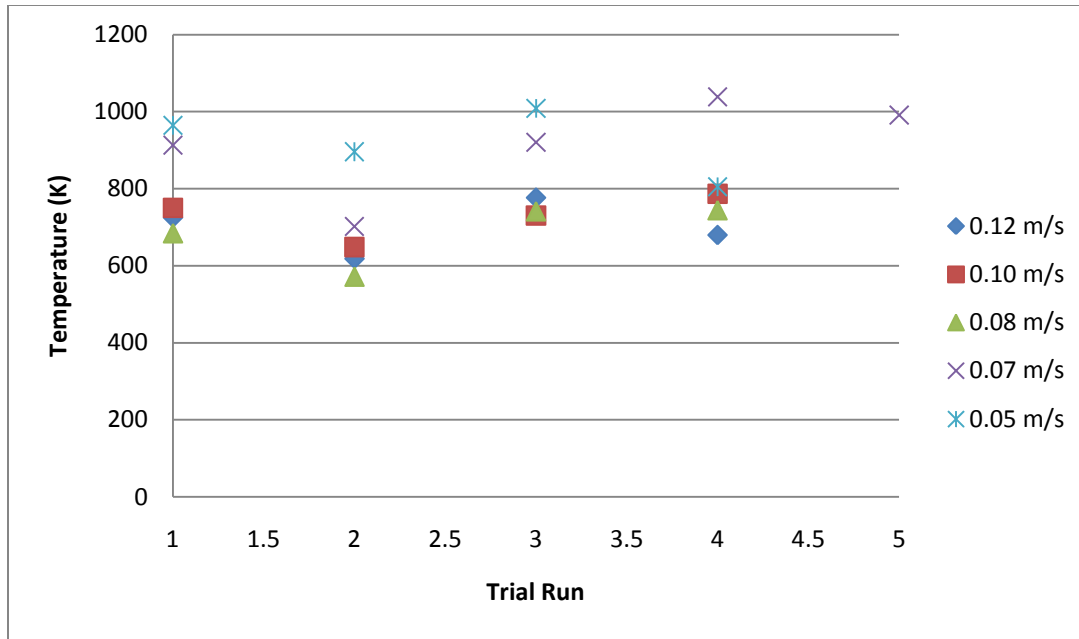


Figure 15: Gas Flame Velocity vs Temperature for an Equivalence Ratio of 0.78

Figure 16 shows the temperatures for the given velocities over a certain amount of trial runs and an equivalence ratio of 1.16. The same trend that is present in the two previous figures is also seen in this one. However, the temperatures for the run at 0.07 m/s are generally 200-300 K higher than in the other two previous figures.

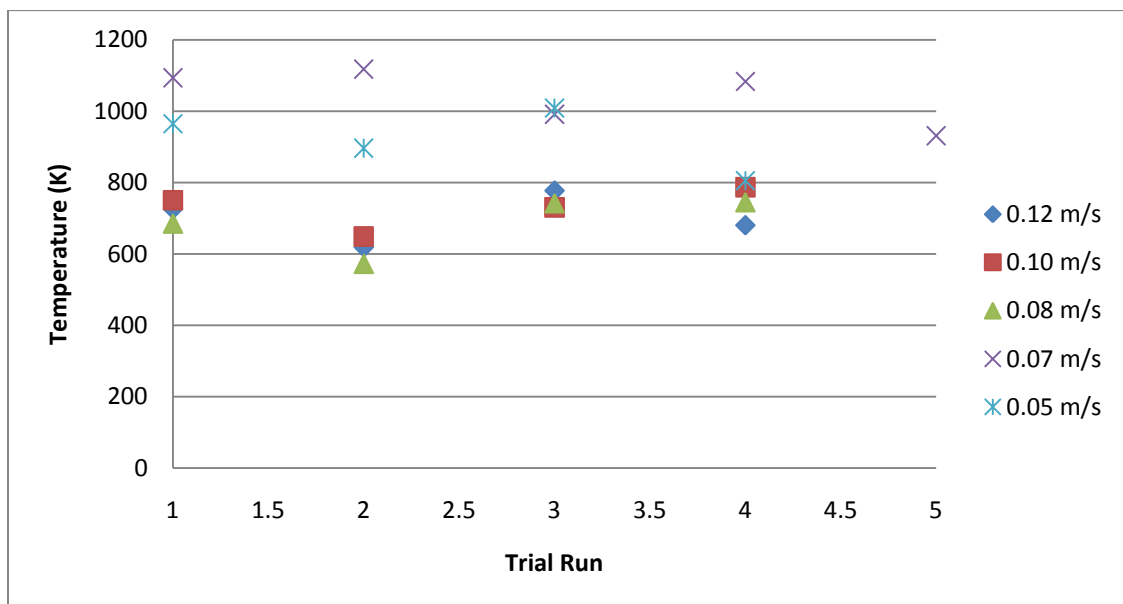


Figure 16: Gas Flame Velocity vs Temperature for an Equivalence Ratio of 1.16

Figure 17 shows the temperatures for the given velocities over a certain amount of trial runs and an equivalence ratio of 1.37. However, there does not appear to be any noticeable trends in this figure. The velocities of 0.12, 0.10, 0.08, and 0.07 m/s seem to vary greatly between trial runs and do not show any trend. However, with the velocity of 0.05 m/s, the temperature appeared relatively constant compared to the other velocities which can be attributed to the thermocouple and its preparation for the experiments during these runs. It was noticed at the end of the set of runs at a velocity of 0.07 m/s that the thermocouple had melted and was producing unreliable temperature readings. Upon replacement, for the set of runs at 0.05 m/s, the temperature readings became more constant and thus more reliable.

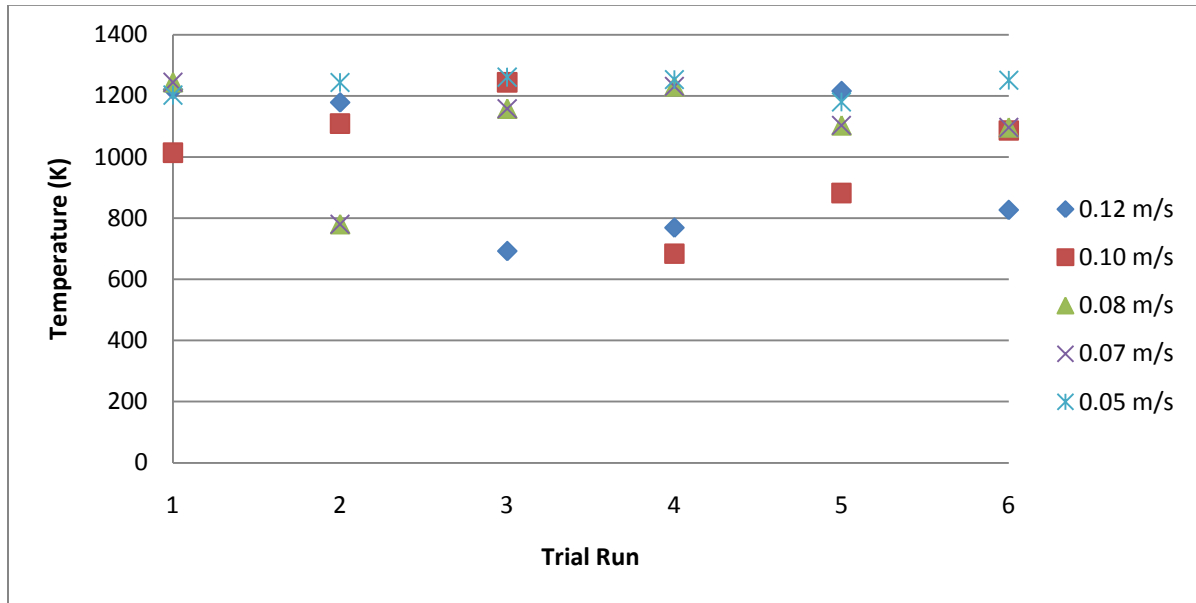


Figure 17: Gas Flame Velocity vs Temperature for an Equivalence Ratio of 1.37

## 4.0 Analysis

### 4.1 Steady-State Preheating

To determine if the experimental procedure for the preheating experiment was accurate, it was compared to the theoretical model that was developed in Section 2.1.3. This section discussed the minimum distance at which heat is felt. Based on the literature, at a heat flux of 1700 W, pain is felt by human skin. The heat flux can be calculated from a view factor, which is the amount of radiation that leaves one surface and strikes another, and is dependent on the specific geometry case. Distance is included in the equation for the view factor, which means that multiple iterations can be performed to determine the minimum distance at which pain is felt. The theoretical distance was determined using this method and was found to be 0.164 m. The experimental distance was determined by holding a thermocouple far enough away from the gas flame that no change in temperature was noticed. The thermocouple was slowly moved closer until a change in temperature was noticed. This distance was 0.191 m, which compares rather favorably to the theoretically determined critical distance of 0.164 m, with only a difference of approximately 3 cm between the two values.

### 4.2 Gas Velocity

The theoretical temperature of the skin for the different velocities wasn't determined due to the fact that low velocities were experimented with. In the theoretical model, the theoretical temperature of the skin was determined for seven different velocities, ranging from 0.1 to 10 m/s. The theoretical temperatures of the skin that were calculated ranged from 35 °C (at 10 m/s) to 900 °C (at 0.1 m/s). Because the velocities that were used in the experiment ranged from 0.12 m/s to 0.05 m/s, reasonable comparisons could not be made.

An important note is that the dust flame velocities were not tested. This is attributed to the instability of the dust flame as well as measurements were only able to be taken through the diffusive part of the dust flame. The dust flame had to be reignited after 20-30 seconds, because it was not

sustainable regardless of the equivalence ratio or amount of dust in the flame. Results were obtained for the steady-state preheating because the measurements could be taken in rapid succession rather than waiting for the arm of the SMA to move at a certain velocity for the velocity experiments.

#### **4.3 Measurement Error**

For the gas flame velocity experiments, the majority of the errors were caused by the software for reading the thermocouple temperature. The software was able to take continuous readings of the temperature for a given length of time; however, the problem that arose from this was the frequency at which these readings were taken. The software was able to take readings at a frequency of 2 Hz, meaning two readings per second. This became an apparent problem for the faster velocities, because the readings were not taken directly in the flame and thus the readings were not accurate. Because these temperature readings were too unreliable to be used, only the five slowest velocities were used.

#### **4.4 Stationary and Moving Flame**

For these experiments, a stationary flame with a moving thermocouple was used instead of moving flame in order to produce a standard testing method, repeatable results and reduce the hazard of testing. If the heat transfer is different between the moving flame and stationary flame, then there will be a difference between the heat flux between the stationary and moving flame. This difference in heat flux could cause either an increase or decrease in the temperatures measured experimentally. However, the differences in heat transfer between turbulent and laminar flames were assumed to be negligible.

#### **4.5 Dust and Gas Flame**

The key difference between dust and gas flames is that dust flames include heat transfer from the dust particles when they deposit on the surface of the skin. Gas flames only include convective and

radiative heat transfer. The action of dust particles sticking to the skin and burning can cause extra damage. In these experiments, this mechanism is not accounted for.

## **5.0 Conclusions**

As shown conceptually and experimentally, it can be concluded that as the velocity decreases the amount of damage to skin increases exponentially. Exposure to a flame front for longer periods of time increases the amount of heat transfer that occurs.

The experimentation done in this project only takes heat transfer by radiation and convection into account. By not accounting for the sticking of dust particles on skin into the analysis, the experimentation was not able to simulate the full amount of damage done by the particulates in a dust flame. However, it can be inferred that the dust flame causes more damage to skin because of the additional heat transfer by conduction from the particulates that could potentially stick to the skin.



## 6.0 Recommendations

For future experimentations, there are multiple areas from this experiment that could be further expanded on to obtain better and more accurate results. For thermocouples, a ceramic rod should be placed up until where the two wires are joined by the bead. This will prevent the two wires from melting and making the readings variable and unreliable. For future experimentations, equipment that can simulate faster velocities would provide better results. As mentioned in Section 4.2, the slower velocities are not a reliable comparison to a dust flame. As indicated in our theoretical models, the preheat temperature of the skin is extremely high, and unreliable. If faster velocities are tested, then the data would be more realistic to what type of damage a dust flame can cause. With testing the faster velocities, equipment that can accurately read the data would further help future experimentations. As mentioned in Section 4.3, the equipment could only accurately read the five slower velocities because of its readings were at a low frequency. If equipment was used that could take readings at higher efficiencies, a wider range of data could be collected.

There are also certain steps that can be taken to improve the dust flame experiments. The most important recommendation for the dust flame experiments would be the ability to create a sustainable dust flame. With a sustainable dust flame, the experiments that were done with a gas flame could be reliably repeated for a dust flame. This would help in drawing a direct comparison between a dust flame and the damage that it does to the human skin rather than comparing a gas flame and the damage it does to the human skin. Another area to improve upon would be the volumetric flow rate for the dust flame. Due to the setup that was available, there was a limited volumetric flow rate range in which testing could be done. Because the flow rate was not high enough, the dust particles were not able to pass through the cone of the flame, which made the results less reliable. At higher volumetric flow rates, this should not be an area of concern. Adjusting the concentration of the dust is also another

recommendation that could help provide more reliable results. With different concentrations of dust, the damage to the skin can be found for different concentrations, and could possibly be applicable for different types of dust explosions rather than only a select few. Along with improving the dust flame, a more in-depth analysis of the particulates should be completed. By studying the dust particulates in-depth, a more defined conclusion can be reached on the damage that the dust flame causes to the human skin.

Another recommendation for future experiments would be to account for the conduction from a dust flame. This is a critical part of the analysis of the damage that a dust flame does to the skin. This is because the conduction element of heating is the reason dust flames cause more damage to the human skin than a gas flame. By being able to accurately determine the conduction from a dust flame, future experiments would have much more definitive proof that dust flames do cause more damage to the skin than a gas flame. One possible way for this to be accomplished would be to use a total heat flux gage that could measure the conduction.

## References

1. "Atex :: GFI Enterprises." *GFI Enterprises :: International Supply Specialists*. Web. 27 May 2010. <<http://www.gfienterprises.co.uk/Atex.html>>.
2. Committee on Evaluation of Industrial Hazards. "A. Classification of Dusts Relative to Electrical Equipment in Class II Hazardous Locations." *National Academies Press* (1982): 1-52. *National Academies Press*. Web. 30 May 2010. <[http://www.nap.edu/openbook.php?record\\_id=10952&page=R1](http://www.nap.edu/openbook.php?record_id=10952&page=R1)>.
3. "Factoids." *Manufacturer of Industrial Gases and Specialty Chemicals--Air Products and Chemicals, Inc*. Web. 13 June 2010. <<http://www.airproducts.com/products/merchantgases/oxygen/factoids.htm>>.
4. *NFPA 654 Standard for the Prevention of Fire and Dust Explosions from the Manufacturing, Processing, and Handling of Combustible Particulate Solids*. Quincy, MA: National Fire Protection Association, 2005. Print.
5. Scott, Jamison. "Explosive: Combustible Dust Issue." *Woodworking Network*. 08 Feb. 2010. Web. 27 June 2010. <[http://woodworkingnetwork.com/Explosive--combustible-dust-issue/2010-02-08/Article.aspx?oid=984661&fid=WWN-ARTICLES&hq\\_e=el&hq\\_m=625822&hq\\_l=10&hq\\_v=051a3e8676](http://woodworkingnetwork.com/Explosive--combustible-dust-issue/2010-02-08/Article.aspx?oid=984661&fid=WWN-ARTICLES&hq_e=el&hq_m=625822&hq_l=10&hq_v=051a3e8676)>.
6. "What Is the Definition of Combustible Dust?" *Online Training from Tooling U*. Web. 27 May 2010. <<http://www.toolingu.com/definition-850190-19410-combustible-dust.html>>.
7. "Explosion Protection - CV TECHNOLOGY." *Explosion Protection Prevention And Mitigation of Dust Hazard - CV TECHNOLOGY*. 2008. Web. 28 June 2010. <<http://www.cvtechnology.com/Explosion-Protection.htm>>.
8. Maness, James E. "GRAIN INDUSTRY'S APPROACH TO DUST EXPLOSIONS." 1-9. Print.
9. "Fire Prevention and Safety During Surgical Procedures." *Valleylab Institute of Clinical Education*. Web. 27 June 2010. <<http://www.valleylabeducation.org/fire/pages/fire-12.html>>.
10. Wieczorek, Christopher J., and Nicholas A. Dembsey. "Human Variability Correction Factors for Use with Simplified Engineering Tools for Predicting Pain and Second Degree Skin Burns." *Journal of Fire Protection Engineering* 2.May 2001 (2001): 88-111. Print.
11. Torodov, G. "Skin Collagen: More than Meets the Eye." *Smart Skin Care - Intelligent Rejuvenation Through Science*. 2010. Web. 7 June 2010. <[http://www.smartskinicare.com/skinbiology/skinbiology\\_collagen.html](http://www.smartskinicare.com/skinbiology/skinbiology_collagen.html)>.
12. Chen, Xu-Lin, Yong-Jie Wang, Chang-Rong Wang, De-Lin Hu, Ye-Xiang Sun, and Shou-Sheng Li. "Burns Due to Gunpowder Explosions in Fireworks Factory: a 13-year Retrospective Study." *Burns* 28.3 (2002): 245-49. Web.
13. Francasso, T., H. Pfeiffer, P. Pellerin, and B. Karger. "The Morphology of Cutaneous Burn Injuries and the Type of Heat Application." *Forensic Science International* (2009): 81-86. Web.
14. Still, J. M., E. J. Law, and H. C. Pickens. "Burns Due to a Sawdust Explosion." *Burns* 22.2 (1996): 164-65. Web.
15. Brannon, From Heather. "Epidermis." *Dermatology - Guide to Skin Conditions and Skin Care*. 18 Feb. 2007. Web. 03 Aug. 2010. <<http://dermatology.about.com/cs/skinanatomy/g/epidermis.htm>>.
16. Brannon, From Heather. "Skin - Anatomy - Skin Layers." *Dermatology - Guide to Skin Conditions and Skin Care*. 09 Apr. 2007. Web. 03 Aug. 2010. <<http://dermatology.about.com/cs/skinanatomy/a/anatomy.htm>>.
17. "16.4 Thermal Resistance Circuits." *MIT*. Web. 31 July 2010. <<http://web.mit.edu/16.unified/www/FALL/thermodynamics/notes/node118.html>>.

18. Chudler, Eric H. "Brain Facts and Figures." *UW Faculty Web Server*. 12 July 2010. Web. 16 Aug. 2010. <<http://faculty.washington.edu/chudler/facts.html>>.
19. "The Weight of Human Skin — Infoplease.com." *Infoplease: Encyclopedia, Almanac, Atlas, Biographies, Dictionary, Thesaurus. Free Online Reference, Research & Homework Help*. — *Infoplease.com*. 2007. Web. 16 Aug. 2010. <<http://www.infoplease.com/askeds/weight-human-skin.html#axzz0wnZ5Y4JV>>.
20. Koehler, Kenneth R. "College Physics for Students of Biology and Chemistry - Heat Flow." *University of Cincinnati, Raymond Walters College*. 2008. Web. 16 Aug. 2010. <<http://www.rwc.uc.edu/koehler/biophys.2ed/heat.html>>.
21. Ratovoson, Domoina, Franck Jourdan, and Vincent Huon. "A Study of Heat Distribution in Human Skin: Use of Infrared Thermography." Web. 14 Aug. 2010. <[http://www.epj-conferences.org/index.php?option=com\\_article&access=standard&Itemid=129&url=/articles/epjconf/pdf/2010/05/epjconf\\_ICEM14\\_21008.pdf](http://www.epj-conferences.org/index.php?option=com_article&access=standard&Itemid=129&url=/articles/epjconf/pdf/2010/05/epjconf_ICEM14_21008.pdf)>.
22. Incropera, Frank P., and David P. DeWitt. "The Semi-Infinite Solid." *Fundamentals of Heat and Mass Transfer*. Hoboken, NJ: John Wiley, 2007. 283-90. Print.
23. Chung, B.T.F. and Sumitra, P.S., 1972, "Radiation shape factors from plane point sources," *J. Heat Transfer*, vol. 94, no. 3, pp. 328-330, August.
24. Zalosh, Robert. "Explosion Protection." *SFPE Handbook of Fire Protection Engineering*. Quincy, MA: National Fire Protection Association, 2008. 3-418--439. Print.
25. Xie, Y., V. Raghavan, and A. S. Rangwala. "Study of Interaction of Entrained Coal Dust Particles in Lean Methane – Air Premixed Flames." Print.

# Appendix

## Appendix A: Skin Density Calculation

Average Human Body Weight: 60 kg

Skin weighs 9lbs = 4.08233 kg

Average area of skin is 22 ft<sup>2</sup> = 2.04386688 m<sup>2</sup>

Thickness to basal layer ( $x_b$ ): 0.08mm =  $8 * 10^{-5}$  m

$$Volume = Area * x_b$$

Volume of skin:  $1.635 * 10^{-4}$  m<sup>3</sup>

$$\rho = mass/volume$$

Density of skin: 24,968 kg/m<sup>3</sup>

## Appendix B: Table of Values

Table 3: Values Used to Calculate Basal Layer Temperature

<b>Density (<math>\rho</math>)</b>		<b>Thermal Conductivity (Heating) <math>k_h</math></b>	
	24,968		0.5878
<b>Heat capacity (<math>c_p</math>)</b>		<b>Thermal Conductivity (Cooling) <math>k_c</math></b>	
	3.558		0.4518
<b>Heat flux (<math>q_1</math>)</b>		<b>Exposure time in seconds (<math>\tau</math>)</b>	
	5		5
<b>Heat flux (<math>q_2</math>)</b>		<b>Basal layer depth (<math>x_b</math>)</b>	
	10		0.00008
<b>Heat flux (<math>q_3</math>)</b>		<b>Initial Temperature in Celsius (<math>T_0</math>)</b>	
	20		32.5
<b>Thermal diffusivity for heating (<math>\alpha_h</math>)</b>		<b>Pi</b>	
	6.61668E-06		3.1415
<b><math>q_1/k_h</math></b>		<b>Thermal diffusivity for cooling (<math>\alpha_c</math>)</b>	
	8.506294658		5.08577E-06
<b><math>q_2/k_h</math></b>		<b><math>q_1/k_c</math></b>	
	17.01258932		11.06684374
<b><math>q_3/k_h</math></b>		<b><math>q_2/k_c</math></b>	
	34.02517863		22.13368747
		<b><math>q_3/k_c</math></b>	
			44.26737494

## Appendix C: Temperature of the Basal Layers with fluxes q1, q2, and q3

Table 4: Basal Layer Temperature Calculated for 60 Seconds

Time in seconds	Temperature of the basal layer with incident heat flux of 5 Watts
10	32.6181081
15	32.67033989
20	32.70817955
25	32.73977139
30	32.76753065
35	32.79260847
40	32.81566798
45	32.83713466
50	32.85730159
55	32.87638117
60	32.89453325
Temperature of the basal layer with incident heat flux of 10 Watts	Temperature of the basal layer with incident heat flux of 20 Watts
32.73621619	32.97243238
32.84067978	33.18135957
32.9163591	33.33271819
32.97954278	33.45908556
33.03506129	33.57012258
33.08521694	33.67043389
33.13133596	33.76267192
33.17426931	33.84853863
33.21460319	33.92920638
33.25276234	34.00552467
33.28906649	34.07813298

## Appendix D: Critical Distance at which Pain is Felt

<b>Stefan-Boltzmann Constant (W/m<sup>2</sup>*K<sup>4</sup>)</b>	<b>n</b>	<b>Emissivity</b>
5.6704E-08	4	0.98
<b>Temperature of Dust Explosion (K)</b>	<b>r (m)</b>	
2000	0.035355339	
<b>Flux from inside a flame</b>	<b>d (m)</b>	
907264	0.025	

<b>D</b>	<b>R</b>	<b>h (m)</b>	<b>View Factor</b>	<b>Heat Flux</b>
0.025	0.035355339	1	0.000795136	706.969947
0.026315789	0.037216146	0.95	0.000880957	783.2757501
0.027777778	0.03928371	0.9	0.000981457	872.6319854
0.029411765	0.041594517	0.85	0.001100182	978.1923195
0.03125	0.044194174	0.8	0.001241818	1104.12347
0.033333333	0.047140452	0.75	0.00141266	1256.022145
0.035714286	0.050507627	0.7	0.001621321	1441.546688
0.038461538	0.054392829	0.65	0.001879839	1671.399688
0.041666667	0.058925565	0.6	0.002205446	1960.903241
0.045454545	0.064282435	0.55	0.002623511	2332.613179
0.05	0.070710678	0.5	0.003172619	2820.835034
0.055555556	0.07856742	0.45	0.003913765	3479.801597
0.0625	0.088388348	0.4	0.004947975	4399.33687
0.071428571	0.101015254	0.35	0.006452432	5736.978468
0.083333333	0.11785113	0.3	0.008761118	7789.673812
0.1	0.141421356	0.25	0.012565343	11172.08175
0.125	0.176776695	0.2	0.01948934	17328.33689
0.166666667	0.23570226	0.15	0.034107801	30325.88421
0.25	0.353553391	0.1	0.073479802	65332.26743
0.5	0.707106781	0.05	0.239463533	212911.5098



D	R	h (m)	View Factor	Heat Flux
0.038462	0.054393	0.65	0.001879839	1671.399688
0.038521	0.054477	0.649	0.001885625	1676.544172
0.03858	0.054561	0.648	0.001891437	1681.712429
0.03864	0.054645	0.647	0.001897277	1686.904605
0.0387	0.05473	0.646	0.001903144	1692.120848
0.03876	0.054814	0.645	0.001909038	1697.361307
0.03882	0.0549	0.644	0.001914959	1702.626131
0.03888	0.054985	0.643	0.001920908	1707.915473
0.038941	0.055071	0.642	0.001926885	1713.229484
0.039002	0.055157	0.641	0.00193289	1718.568317
0.039063	0.055243	0.64	0.001938922	1723.932129

D	R	h (m)	View Factor	Heat Flux
0.03876	0.054814	0.645	0.001909038	1697.361307
0.038766	0.054823	0.6449	0.001909629	1697.88669
0.038772	0.054831	0.6448	0.00191022	1698.412318
0.038778	0.05484	0.6447	0.001910811	1698.938189
0.038784	0.054848	0.6446	0.001911403	1699.464304
0.03879	0.054857	0.6445	0.001911995	1699.990664
0.038796	0.054866	0.6444	0.001912587	1700.517268
0.038802	0.054874	0.6443	0.00191318	1701.044117
0.038808	0.054883	0.6442	0.001913773	1701.57121
0.038814	0.054891	0.6441	0.001914366	1702.098548
0.03882	0.0549	0.644	0.001914959	1702.626131

## Appendix E: Preheat Temperature

<b>density (rho)</b>	<b>Thermal Conductivity (Heating) kh</b>
24,968	0.5878
<b>heat capacity (cp)</b>	<b>Thermal Conductivity (Cooling) kc</b>
3558	0.4518
<b>Thermal diffusivity for heating (alpha h)</b>	
6.61668E-09	
<b>Thermal diffusivity for cooling (alpha c)</b>	<b>Basal layer depth (xb)</b>
5.08577E-09	0.00008
<b>Pi</b>	<b>Average Initial Temperature in Kelvin (T0)</b>
3.1415	305.5

**Velocity = 1 m/s**

Time	Exposure time	Heat Flux	q1/kh	q1/kc	Temperature
0.981576	0.017887886	46427.81937	78985.742	102761.8844	53.29285525

Time (s)	Exposure time (s)	Heat flux at 1 m/s (q1)	q1/kh	q1/kc
0.3555	0.018414	1699.991	2892.124	3762.706
0.373914286	0.018414	1801.245	3064.385	3986.820
0.392328571	0.018414	1911.816	3252.495	4231.555
0.410742857	0.018414	2032.881	3458.458	4499.516
0.429157143	0.018414	2165.811	3684.605	4793.738
0.447571429	0.018414	2312.205	3933.659	5117.762
0.465985714	0.018414	2473.944	4208.819	5475.751
0.4844	0.018414	2653.248	4513.862	5872.616
0.502814286	0.018414	2852.752	4853.270	6314.192
0.521228571	0.018414	3075.605	5232.400	6807.447
0.539642857	0.018414	3325.592	5657.692	7360.760
0.558057143	0.018414	3607.296	6136.945	7984.277
0.576471429	0.018414	3926.312	6679.673	8690.376
0.594885714	0.018414	4289.518	7297.581	9494.286
0.6133	0.018414	4705.454	8005.195	10414.905
0.631714286	0.018414	5184.819	8820.720	11475.917
0.650128571	0.018414	5741.167	9767.212	12707.320
0.668542857	0.018414	6391.862	10874.213	14147.548
0.686957143	0.018414	7159.441	12180.063	15846.483
0.705371429	0.018414	8073.570	13735.233	17869.788
0.723785714	0.018414	9173.922	15607.217	20305.272
0.7422	0.018414	10514.498	17887.884	23272.462
0.760614286	0.018414	12170.283	20704.803	26937.325
0.779028571	0.018414	14247.779	24239.161	31535.589
0.797442857	0.018414	16902.220	28755.052	37410.844
0.815857143	0.018414	20366.728	34649.078	45079.080
0.834271429	0.018414	25003.792	42537.924	55342.611
0.852685714	0.018414	31400.598	53420.547	69501.101
0.8711	0.018414	40555.777	68995.878	89764.889
0.889514286	0.018414	54269.873	92327.106	120119.240
0.907928571	0.018414	76026.048	129339.993	168273.678
0.926342857	0.018414	113150.425	192498.171	250443.614
0.944757143	0.018414	182528.944	310528.997	404003.861
0.963171429	0.018414	325379.674	553555.077	720185.202
0.981585714	0	617898.59	1051205.49	1367637.42

**Velocity = 5 m/s**

Time	Exposure time	Heat Flux	q2/kh	q2kc	Temperature
0.196315	0.003577577	9285.563875	15797.148	20552.37688	38.43050002

Time (s)	Exposure time (s)	Heat flux at 5 m/s (q2)	q2/kh	q2/kc
0.0711	0.0036828	339.9981328	578.4248602	752.5412413
0.074782857	0.0036828	360.2490955	612.8769914	797.3640893
0.078465714	0.0036828	382.3632863	650.4989559	846.3109479
0.082148571	0.0036828	406.5762959	691.6915547	899.9032667
0.085831429	0.0036828	433.1621291	736.9209411	958.7475191
0.089514286	0.0036828	462.4409664	786.7318245	1023.552382
0.093197143	0.0036828	494.7888163	841.763893	1095.150102
0.09688	0.0036828	530.6496047	902.7723795	1174.523251
0.100562857	0.0036828	570.5504281	970.6540117	1262.838486
0.104245714	0.0036828	615.1209531	1046.480016	1361.489493
0.107928571	0.0036828	665.1183004	1131.538449	1472.152059
0.111611429	0.0036828	721.4592559	1227.389003	1596.855369
0.115294286	0.0036828	785.2623802	1335.934638	1738.075211
0.118977143	0.0036828	857.9036428	1459.516235	1898.857111
0.12266	0.0036828	941.0907747	1601.039086	2082.980909
0.126342857	0.0036828	1036.96388	1764.144063	2295.183445
0.130025714	0.0036828	1148.233444	1953.442402	2541.464019
0.133708571	0.0036828	1278.372448	2174.842546	2829.509625
0.137391429	0.0036828	1431.888219	2436.012622	3169.296634
0.141074286	0.0036828	1614.714013	2747.046636	3573.957532
0.144757143	0.0036828	1834.784414	3121.443372	4061.05448
0.14844	0.0036828	2102.899686	3577.576873	4654.492443
0.152122857	0.0036828	2434.056658	4140.96063	5387.464936
0.155805714	0.0036828	2849.555785	4847.83223	6307.117718
0.159488571	0.0036828	3380.443908	5751.010391	7482.168898
0.163171429	0.0036828	4073.345658	6929.815682	9015.815976
0.166854286	0.0036828	5000.758304	8507.584729	11068.52214
0.170537143	0.0036828	6280.119521	10684.10943	13900.22028
0.17422	0.0036828	8111.155361	13799.1755	17952.97778
0.177902857	0.0036828	10853.97454	18465.42113	24023.84803
0.181585714	0.0036828	15205.20953	25867.99851	33654.73556
0.185268571	0.0036828	22630.08499	38499.63422	50088.72287
0.188951429	0.0036828	36505.78887	62105.79937	80800.77218
0.192634286	0.0036828	65075.93487	110711.0154	144037.0404
0.196317143	0	123579.7175	210241.0981	273527.4844

**Velocity = 10 m/s**

Time	Exposure time	Heat Flux	q3/kh	q3/kc	Temperature
0.191408	0.001788789	4642.781937	7898.5742	10276.18844	35.51163593

Time (s)	Exposure time (s)	Heat flux at 10 m/s (q3)	q3/kh	q3/kc
0.03555	0.0018414	169.9990664	289.2124301	376.2706206
0.037391429	0.0018414	180.1245478	306.4384957	398.6820446
0.039232857	0.0018414	191.1816431	325.2494779	423.155474
0.041074286	0.0018414	203.2881479	345.8457774	449.9516333
0.042915714	0.0018414	216.5810646	368.4604705	479.3737596
0.044757143	0.0018414	231.2204832	393.3659122	511.7761912
0.046598571	0.0018414	247.3944081	420.8819465	547.5750512
0.04844	0.0018414	265.3248023	451.3861897	587.2616253
0.050281429	0.0018414	285.275214	485.3270058	631.4192431
0.052122857	0.0018414	307.5604766	523.2400078	680.7447467
0.053964286	0.0018414	332.5591502	565.7692245	736.0760296
0.055805714	0.0018414	360.7296279	613.6945014	798.4276847
0.057647143	0.0018414	392.6311901	667.967319	869.0376053
0.059488571	0.0018414	428.9518214	729.7581174	949.4285556
0.06133	0.0018414	470.5453873	800.5195429	1041.490454
0.063171429	0.0018414	518.4819402	882.0720316	1147.591722
0.065012857	0.0018414	574.1167218	976.7212008	1270.732009
0.066854286	0.0018414	639.1862242	1087.421273	1414.754812
0.068695714	0.0018414	715.9441097	1218.006311	1584.648317
0.070537143	0.0018414	807.3570064	1373.523318	1786.978766
0.072378571	0.0018414	917.392207	1560.721686	2030.52724
0.07422	0.0018414	1051.449843	1788.788436	2327.246222
0.076061429	0.0018414	1217.028329	2070.480315	2693.732468
0.077902857	0.0018414	1424.777892	2423.916115	3153.558859
0.079744286	0.0018414	1690.221954	2875.505196	3741.084449
0.081585714	0.0018414	2036.672829	3464.907841	4507.907988
0.083427143	0.0018414	2500.379152	4253.792365	5534.261071
0.085268571	0.0018414	3140.05976	5342.054713	6950.110138
0.08711	0.0018414	4055.57768	6899.587752	8976.48889
0.088951429	0.0018414	5426.987269	9232.710563	12011.92401
0.090792857	0.0018414	7602.604763	12933.99926	16827.36778
0.092634286	0.0018414	11315.0425	19249.81711	25044.36144
0.094475714	0.0018414	18252.89444	31052.89969	40400.38609
0.096317143	0.0018414	32537.96744	55355.50772	72018.52022
0.098158571	0	61789.85873	105120.549	136763.7422

**Velocity = 3 m/s**

Time	Exposure time	Heat Flux	q4/kh	q4/kc	Temperature
0.327192	0.005962629	15475.93979	26328.581	34253.96147	39.54178592

Time (s)	Exposure time (s)	Heat flux at 3 m/s (q4)	q4/kh	q4/kc
0.1185	0.006138	566.6635547	964.0414336	1254.235402
0.124638	0.006138	600.4151592	1021.461652	1328.940149
0.130776	0.006138	637.2721438	1084.164926	1410.518247
0.136914	0.006138	677.6271598	1152.819258	1499.838778
0.143052	0.006138	721.9368819	1228.201568	1597.912532
0.14919	0.006138	770.734944	1311.219707	1705.920637
0.155328	0.006138	824.6480271	1402.939822	1825.250171
0.161466	0.006138	884.4160078	1504.620632	1957.538751
0.167604	0.006138	950.9173801	1617.756686	2104.73081
0.173742	0.006138	1025.201589	1744.133359	2269.149156
0.17988	0.006138	1108.530501	1885.897415	2453.586765
0.186018	0.006138	1202.432093	2045.648338	2661.425616
0.192156	0.006138	1308.770634	2226.55773	2896.792018
0.198294	0.006138	1429.839405	2432.527058	3164.761852
0.204432	0.006138	1568.484624	2668.398476	3471.634848
0.21057	0.006138	1728.273134	2940.240105	3825.305741
0.216708	0.006138	1913.722406	3255.737336	4235.773364
0.222846	0.006138	2130.620747	3624.737577	4715.849375
0.228984	0.006138	2386.480366	4060.021037	5282.161057
0.235122	0.006138	2691.190021	4578.411061	5956.595886
0.24126	0.006138	3057.974023	5202.40562	6768.424133
0.247398	0.006138	3504.83281	5962.628122	7757.487406
0.253536	0.006138	4056.761097	6901.60105	8979.108227
0.259674	0.006138	4749.259642	8079.720384	10511.86286
0.265812	0.006138	5634.07318	9585.017319	12470.2815
0.27195	0.006138	6788.90943	11549.6928	15026.35996
0.278088	0.006138	8334.597173	14179.30788	18447.5369
0.284226	0.006138	10466.86587	17806.84904	23167.03379
0.290364	0.006138	13518.59227	22998.62584	29921.62963
0.296502	0.006138	18089.95756	30775.70188	40039.74671
0.30264	0.006138	25342.01588	43113.33086	56091.22594
0.308778	0.006138	37716.80832	64166.05703	83481.20479
0.314916	0.006138	60842.98145	103509.6656	134667.9536
0.321054	0.006138	108459.8915	184518.3591	240061.7341
0.327192	0	205966.1958	350401.8301	455879.1407

**Velocity = 0.5 m/s**

Time	Exposure time	Heat Flux	q5/kh	q5/kc	Temperature
1.963152	0.035775771	157971.4848	268750.4	349649.1473	119.9064113

Time (s)	Exposure time (s)	Heat flux at 0.5 m/s (q5)	q5/kh	q5/kc
0.711	0.036828	5784.248602	9840.504596	12802.67508
0.747828	0.036828	6128.769914	10426.62456	13565.22779
0.784656	0.036828	6504.989559	11066.67159	14397.94059
0.821484	0.036828	6916.915547	11767.46435	15309.6847
0.858312	0.036828	7369.209411	12536.93333	16310.7778
0.89514	0.036828	7867.318245	13384.34543	17413.27633
0.931968	0.036828	8417.63893	14320.58341	18631.33893
0.968796	0.036828	9027.723795	15358.49574	19981.68171
1.005624	0.036828	9706.540117	16513.33807	21484.15254
1.042452	0.036828	10464.80016	17803.33473	23162.46161
1.07928	0.036828	11315.38449	19250.39893	25045.11839
1.116108	0.036828	12273.89003	20881.06504	27166.6446
1.152936	0.036828	13359.34638	22727.70735	29569.15976
1.189764	0.036828	14595.16235	24830.1503	32304.4762
1.226592	0.036828	16010.39086	27237.82045	35436.89876
1.26342	0.036828	17641.44063	30012.65844	39047.01335
1.300248	0.036828	19534.42402	33233.11333	43236.88361
1.337076	0.036828	21748.42546	36999.70306	48137.28521
1.373904	0.036828	24360.12622	41442.88231	53917.94206
1.410732	0.036828	27470.46636	46734.37626	60802.27172
1.44756	0.036828	31214.43372	53103.83416	69089.05205
1.484388	0.036828	35775.76873	60863.84609	79184.96841
1.521216	0.036828	41409.6063	70448.46257	91654.72842
1.558044	0.036828	48478.3223	82474.17881	107300.4035
1.594872	0.036828	57510.10391	97839.57794	127291.0667
1.6317	0.036828	69298.15682	117894.1082	153382.3746
1.668528	0.036828	85075.84729	144736.0451	188304.2215
1.705356	0.036828	106841.0943	181764.3659	236478.739
1.742184	0.036828	137991.755	234759.7057	305426.638
1.779012	0.036828	184654.2113	314144.6262	408707.8602
1.81584	0.036828	258679.9851	440081.6352	572554.1947
1.852668	0.036828	384996.3422	654978.4658	852138.8716
1.889496	0.036828	621057.9937	1056580.459	1374630.354
1.926324	0.036828	1107110.154	1883481.038	2450443.015
1.963152	0	2102410.981	3576745.459	4653410.759

**Velocity = 0.2 m/s**

Time	Exposure time	Heat Flux	q6/kh	q6/kc	Temperature
4.90788	0.089439429	394928.7119	671876	874122.8684	349.6316043

Time (s)	Exposure time (s)	Heat flux at 0.2 m/s (q6)	q6/kh	q6/kc
1.7775	0.09207	14460.6215	24601.26149	32006.6877
1.86957	0.09207	15321.92478	26066.56139	33913.06947
1.96164	0.09207	16262.4739	27666.67897	35994.85148
2.05371	0.09207	17292.28887	29418.66089	38274.21175
2.14578	0.09207	18423.02353	31342.33332	40776.9445
2.23785	0.09207	19668.29561	33460.86358	43533.19082
2.32992	0.09207	21044.09732	35801.45853	46578.34733
2.42199	0.09207	22569.30949	38396.23935	49954.20427
2.51406	0.09207	24266.35029	41283.34517	53710.38135
2.60613	0.09207	26162.00039	44508.33683	57906.15402
2.6982	0.09207	28288.46123	48125.99732	62612.79599
2.79027	0.09207	30684.72507	52202.66259	67916.61149
2.88234	0.09207	33398.36595	56819.26837	73922.8994
2.97441	0.09207	36487.90587	62075.37576	80761.19051
3.06648	0.09207	40025.97715	68094.55112	88592.24689
3.15855	0.09207	44103.60158	75031.6461	97617.53338
3.25062	0.09207	48836.06004	83082.78332	108092.209
3.34269	0.09207	54371.06365	92499.25765	120343.213
3.43476	0.09207	60900.31556	103607.2058	134794.8552
3.52683	0.09207	68676.16591	116835.9406	152005.6793
3.6189	0.09207	78036.08429	132759.5854	172722.6301
3.71097	0.09207	89439.42182	152159.6152	197962.421
3.80304	0.09207	103524.0157	176121.1564	229136.821
3.89511	0.09207	121195.8058	206185.447	268251.0088
3.98718	0.09207	143775.2598	244598.9448	318227.6666
4.07925	0.09207	173245.3921	294735.2706	383455.9364
4.17132	0.09207	212689.6182	361840.1127	470760.5539
4.26339	0.09207	267102.7356	454410.9147	591196.8474
4.35546	0.09207	344979.3876	586899.2643	763566.5949
4.44753	0.09207	461635.5281	785361.5654	1021769.651
4.5396	0.09207	646699.9629	1100204.088	1431385.487
4.63167	0.09207	962490.8555	1637446.165	2130347.179
4.72374	0.09207	1552644.984	2641451.147	3436575.884
4.81581	0.09207	2767775.386	4708702.596	6126107.538
4.90788	0	5256027.452	8941863.648	11633526.9



**Velocity = 0.1 m/s**

Time	Exposure time	Heat Flux	q7/kh	q7/kc	Temperature
9.81576	0.178878857	789857.4238	1343752	1748245.737	900.3070774

Time (s)	Exposure time (s)	Heat flux at 0.1 m/s (q7)	q7/kh	q7/kc
3.555	0.18414	28921.24301	49202.52298	64013.37541
3.73914	0.18414	30643.84957	52133.12278	67826.13893
3.92328	0.18414	32524.94779	55333.35794	71989.70295
4.10742	0.18414	34584.57774	58837.32177	76548.4235
4.29156	0.18414	36846.04705	62684.66664	81553.88901
4.4757	0.18414	39336.59122	66921.72716	87066.38163
4.65984	0.18414	42088.19465	71602.91706	93156.69466
4.84398	0.18414	45138.61897	76792.47869	99908.40853
5.02812	0.18414	48532.70058	82566.69034	107420.7627
5.21226	0.18414	52324.00078	89016.67366	115812.308
5.3964	0.18414	56576.92245	96251.99465	125225.592
5.58054	0.18414	61369.45014	104405.3252	135833.223
5.76468	0.18414	66796.7319	113638.5367	147845.7988
5.94882	0.18414	72975.81174	124150.7515	161522.381
6.13296	0.18414	80051.95429	136189.1022	177184.4938
6.3171	0.18414	88207.20316	150063.2922	195235.0668
6.50124	0.18414	97672.12008	166165.5666	216184.4181
6.68538	0.18414	108742.1273	184998.5153	240686.4261
6.86952	0.18414	121800.6311	207214.4116	269589.7103
7.05366	0.18414	137352.3318	233671.8813	304011.3586
7.2378	0.18414	156072.1686	265519.1708	345445.2603
7.42194	0.18414	178878.8436	304319.2304	395924.8421
7.60608	0.18414	207048.0315	352242.3129	458273.6421
7.79022	0.18414	242391.6115	412370.894	536502.0175
7.97436	0.18414	287550.5196	489197.8897	636455.3333
8.1585	0.18414	346490.7841	589470.5412	766911.8728
8.34264	0.18414	425379.2365	723680.2254	941521.1077
8.52678	0.18414	534205.4713	908821.8294	1182393.695
8.71092	0.18414	689958.7752	1173798.529	1527133.19
8.89506	0.18414	923271.0563	1570723.131	2043539.301
9.0792	0.18414	1293399.926	2200408.176	2862770.973
9.26334	0.18414	1924981.711	3274892.329	4260694.358
9.44748	0.18414	3105289.969	5282902.294	6873151.768
9.63162	0.18414	5535550.772	9417405.192	12252215.08
9.81576	0	10512054.9	17883727.3	23267053.79

## Appendix F: Exposure Time versus Flame Thickness

Assuming the thermocouple is passing through the tip of the flame where it is 2x thick where flame thickness varies between 1mm and 10cm.

Velocity (m/s)	Flame Thickness (mm)	Flame Thickness (m)	Skin Thickness (mm)	Skin Thickness (m)	Total Thickness (m)	Exposure Time (s)
1	2	0.002	2	0.002	0.004	0.004
1	20	0.02	2	0.002	0.022	0.022
1	40	0.04	2	0.002	0.042	0.042
1	60	0.06	2	0.002	0.062	0.062
1	80	0.08	2	0.002	0.082	0.082
1	100	0.1	2	0.002	0.102	0.102
1	120	0.12	2	0.002	0.122	0.122
1	140	0.14	2	0.002	0.142	0.142
1	160	0.16	2	0.002	0.162	0.162
1	180	0.18	2	0.002	0.182	0.182
1	200	0.2	2	0.002	0.202	0.202

Velocity (m/s)	Flame Thickness (mm)	Flame Thickness (m)	Skin Thickness (mm)	Skin Thickness (m)	Total Thickness (m)	Exposure Time (s)
5	2	0.002	2	0.002	0.004	0.0008
5	20	0.02	2	0.002	0.022	0.0044
5	40	0.04	2	0.002	0.042	0.0084
5	60	0.06	2	0.002	0.062	0.0124
5	80	0.08	2	0.002	0.082	0.0164
5	100	0.1	2	0.002	0.102	0.0204
5	120	0.12	2	0.002	0.122	0.0244
5	140	0.14	2	0.002	0.142	0.0284
5	160	0.16	2	0.002	0.162	0.0324
5	180	0.18	2	0.002	0.182	0.0364
5	200	0.2	2	0.002	0.202	0.0404

<b>Velocity (m/s)</b>	<b>Flame Thickness (mm)</b>	<b>Flame Thickness (m)</b>	<b>Skin Thickness (mm)</b>	<b>Skin Thickness (m)</b>	<b>Total Thickness (m)</b>	<b>Exposure Time (s)</b>
10	2	0.002	2	0.002	0.004	0.0004
10	20	0.02	2	0.002	0.022	0.0022
10	40	0.04	2	0.002	0.042	0.0042
10	60	0.06	2	0.002	0.062	0.0062
10	80	0.08	2	0.002	0.082	0.0082
10	100	0.1	2	0.002	0.102	0.0102
10	120	0.12	2	0.002	0.122	0.0122
10	140	0.14	2	0.002	0.142	0.0142
10	160	0.16	2	0.002	0.162	0.0162
10	180	0.18	2	0.002	0.182	0.0182
10	200	0.2	2	0.002	0.202	0.0202

**Appendix G: Temperature of the Basal Layer Updated with the Preheat Temperature, Flux from Inside a Flame, and Velocity**

<b>density (rho)</b>	<b>Thermal Conductivity (Heating) kh</b>
24,968	0.5878
<b>heat capacity (cp)</b>	<b>Thermal Conductivity (Cooling) kc</b>
3558	0.4518
<b>Heat flux (q1)</b>	<b>Exposure time in seconds (tau)</b>
907264	0.004
<b>Heat flux (q2)</b>	<b>Basal layer depth (xb)</b>
181452.8	0.00008
<b>Heat flux (q3)</b>	<b>Pi</b>
90726.4	3.1415
<b>Thermal diffusivity for heating (alpha h)</b>	<b>Thermal diffusivity for cooling (alpha c)</b>
6.61668E-09	5.08577E-09

<b>q1/kc</b>	<b>q1/kh</b>
2008109.783	1543490.983
<b>q2/kc</b>	<b>q2/kh</b>
401621.9566	308698.1967
<b>q3/kc</b>	<b>q3/kh</b>
200810.9783	154349.0983

<b>Stefan-Boltzmann Constant (W/m<sup>2</sup>*K<sup>4</sup>)</b>
5.6704E-08
<b>Temperature of Dust Explosion (K)</b>
2000
<b>Flux from inside a flame</b>
907264

<b>Time in seconds for 1m/s flame</b>	<b>Exposure Time for 1 m/s flame</b>	<b>Temperature of the basal layer of a flame traveling at 1 m/s</b>
0.985576	0.004	461.7443845
1.003576	0.022	461.2485877
1.023576	0.042	460.7131776
1.043576	0.062	460.1931638
1.063576	0.082	459.6877259
1.083576	0.102	459.1961434
1.103576	0.122	458.7177902
1.123576	0.142	458.2521299
1.143576	0.162	457.7987122
1.163576	0.182	457.3571694
1.183576	0.202	456.9272151

<b>Time in seconds for 5 m/s flame</b>	<b>Exposure Time for 5 m/s flame</b>	<b>Temperature of the basal layer of a flame traveling at 5 m/s</b>
0.1971152	0.0008	152.0804038
0.2007152	0.0044	152.2825603
0.2047152	0.0084	152.5884928
0.2087152	0.0124	152.9795042
0.2127152	0.0164	153.4556212
0.2167152	0.0204	154.0174258
0.2207152	0.0244	154.6660428
0.2247152	0.0284	155.4031334
0.2287152	0.0324	156.2309034
0.2327152	0.0364	157.1521124
0.2367152	0.0404	158.1700951

<b>Time in seconds for 10 m/s flame</b>	<b>Exposure Time for 10 m/s flame</b>	<b>Temperature of the basal layer of a flame traveling at 10 m/s</b>
0.1918076	0.0004	96.68319879
0.1936076	0.0022	96.73547728
0.1956076	0.0042	96.80505693
0.1976076	0.0062	96.88666605
0.1996076	0.0082	96.98025668
0.2016076	0.0102	97.08580221
0.2036076	0.0122	97.20329827
0.2056076	0.0142	97.33276137
0.2076076	0.0162	97.47422874
0.2096076	0.0182	97.62775813
0.2116076	0.0202	97.79342757

## Appendix H: Flux Required for Skin Damage and Skin Death

<b>density (rho)</b>	<b>Thermal Conductivity (Heating) kh</b>
24,968	0.5878
<b>heat capacity (cp)</b>	<b>Thermal Conductivity (Cooling) kc</b>
3558	0.4518
<b>Thermal diffusivity for cooling (alpha c)</b>	<b>Exposure time in seconds (tau)</b>
5.08577E-09	5
<b>Thermal diffusivity for heating (alpha h)</b>	<b>Basal layer depth (xb)</b>
6.61668E-09	0.00008
<b>T1 (temperature to injury [44C])</b>	<b>Average Initial Temperature in Kelvin (T0)</b>
317	305.5
<b>T2 (temperature to skin death [72C])</b>	<b>Pi</b>
345	3.1415

<b>Time in seconds</b>	<b>Flux (Watts) required for 44C</b>	<b>Flux (Watts) required for 72C</b>
9	16672.64323	57266.90501
20	8419.11322	28917.82367
40	5625.567768	19322.60233
60	4524.318703	15540.0512
80	3891.612862	13366.84418
100	3467.611802	11910.49271
120	3157.979293	10846.97235
140	2919.030406	10026.23487
160	2727.376131	9367.944102
180	2569.20871	8824.673394
200	2435.779745	8366.373907
220	2321.240797	7972.957519
240	2221.513525	7630.416021

## Appendix I: Servo Motor Velocity

Angle (degrees)	Length (cm)	Time (ms)	Time (s)	Velocity (m/s)
50	33.655	254	0.254	1.16
Arclength (cm)		508	0.508	0.58
29.36866181		762	0.762	0.39
Arclength (m)		1270	1.27	0.23
0.293686618		2032	2.032	0.14
		2540	2.54	0.12
		3048	3.048	0.10
		3556	3.556	0.08
		4318	4.318	0.07
		6350	6.35	0.05



## Appendix J: Correction Factor

### *Appendix J.1: Conduction Correction*

<b>Conduction Correction</b>	
<b>Need a minimum length to diameter ratio of 200</b>	
Diameter (m)	
	0.00016
Length (m)	
	1.8288
Actual length to diameter ratio	
	11430
Conduction negligible	

**Appendix J.2: Convection Correction**

<b>Convective Correction</b>					
	Equivalence Ratio 1	Equivalence Ratio 2	Equivalence Ratio 3	Equivalence Ratio 4	Equivalence Ratio 5
Density	0.2275	0.225625	0.23125	0.229375	0.229725
Viscosity	1.74000E-06	2.15000E-06	9.20000E-07	1.33000E-06	1.12475E-06
Density of Air (kg/m <sup>3</sup> )	Viscosity of Air (Pa*s)				
0.235	0.0000001				
Density of Methane (kg/m <sup>3</sup> )	Viscosity of CH <sub>4</sub> (Pa*s)				
0.16	0.0000165				
	Length				
	0.00635				
<b>Reynolds Number (Re=ρvl/η)</b>					
	Equivalence Ratio 1	Equivalence Ratio 2	Equivalence Ratio 3	Equivalence Ratio 4	Equivalence Ratio 5
Velocity (m/s)					
1.16	959.9670	770.5005	1845.5171	1266.2475	1499.6034
0.58	479.9835	385.2503	922.7586	633.1238	749.8017
0.39	319.9890	256.8335	615.1724	422.0825	499.8678
0.23	119.9959	154.1001	369.1034	253.2495	299.9207
0.14	95.9967	96.3126	230.6896	158.2809	187.4504
0.12	79.9973	77.0501	184.5517	126.6248	149.9603
0.10	68.5691	64.2084	153.7931	105.5206	124.9670
0.08	56.4686	55.0358	131.8227	90.4463	107.1145
0.07	38.3987	45.3236	108.5598	74.4851	88.2120
0.05	38.3987	30.8200	73.8207	50.6499	59.9841

	air	n gas
EQ1	90.00%	10.00%
EQ2	87.50%	12.50%
EQ3	91.25%	8.75%
EQ4	92.50%	7.50%
EQ5	93.75%	6.25%

	$\mu$	cp	k
air	0.00001845	0.001005	0.02587
methane	0.00001114	0.002225	0.03281

<b>Prandtl Number (<math>Pr=c_p\mu/k</math>)</b>					
	Equivalenc e Ratio 1	Equivalenc e Ratio 2	Equivalenc e Ratio 3	Equivalenc e Ratio 4	Equivalenc e Ratio 5
Specific Heat ( $c_p$ ) [J/kg*K]	1.127E+03	1.158E+03	1.112E+03	1.097E+03	1.097E+03
Dynamic Viscosity ( $\mu$ ) [Pa*s]	1.772E-05	1.754E-05	1.781E-05	1.790E-05	1.790E-05
Thermal Conductivity (k) [W/m*K]	2.656E-02	2.674E-02	2.648E-02	2.639E-02	2.639E-02
<b>Prandtl Number (Pr)</b>	7.517E-01	7.592E-01	7.478E-01	7.438E-01	7.438E-01

<b>Nusselt Number [<math>Nu=2+.6(Re^{.5})(Pr^{.33})</math>] for <math>Re&gt;200</math></b>					
	Gas	Gas	Gas	Gas	Dust
Velocity	Equivalenc e Ratio 1	Equivalenc e Ratio 2	Equivalenc e Ratio 3	Equivalenc e Ratio 4	Equivalenc e Ratio 5
1.16	16455.6566	10646.2864	60661.4726	28501.8477	39970.23721
0.58	4120.4681	2667.6173	15173.8611	7132.7418	10000.34927
0.39	1835.3390	1189.3350	6749.0740	3174.5451	4449.330879
0.23	7.9762	8.7946	2434.6086	1147.1429	1606.332907
0.14	7.3453	7.3716	954.9740	8.8394	9.4430
0.12	6.8795	6.8045	9.3985	8.1173	8.6572
0.10	6.5176	6.3859	8.7539	7.5843	8.0772
0.08	6.0996	6.0606	8.2529	7.1701	7.6264
0.07	5.3806	5.6849	7.6744	6.6918	7.1058
0.05	5.3806	5.0386	6.6792	5.8689	6.2104

### Appendix K: Equivalence Ratio Setup

Stoichiometric								
Air Fuel Ratio (AFR)	Volumetric Flow of Air (L/min)	Density of Air (g/L)	Mass of Air (g)	Volumetric Flow of Natural Gas (cc/min)	Density of Natural Gas (g/cc)	Mass of Natural Gas (g)	Percent Natural Gas	Total Flow (cc/min)
17.2	13.49019608	1.275	17.2	1498.911041	0.000667151	1	10.00%	14989.1071

Experimental										
Flame Type	Air Fuel Ratio (AFR)	Vol. Flow of Air (L/min)	Density of Air (g/L)	Mass of Air (g)	Vol. Flow of Nat Gas (cc/min)	Density of Nat Gas (g/cc)	Mass of Nat Gas (g)	% Nat Gas	% Air	Total Flow (cc/min)
Gas	17.20	7.2	1.275	9.18	800	6.672E-04	0.5	10.0%	90.0%	8000
Gas	13.38	7.0	1.275	8.925	1000	6.672E-04	0.7	12.5%	87.5%	8000
Gas	19.93	7.3	1.275	9.3075	700	6.672E-04	0.5	8.8%	91.3%	8000
Gas	23.57	7.4	1.275	9.435	600	6.672E-04	0.4	7.5%	92.5%	8000
Dust	28.67	3.0	1.275	3.825	200	6.672E-04	0.1	6.3%	93.8%	3200

Flame Type	Equivalence Ratio
Gas	1.00
Gas	0.78
Gas	1.16
Gas	1.37
Dust	1.67

**Appendix L: Gas Equivalence Ratio 1 Raw Data**

<b>Preheat</b>					
<b>Distance (in)</b>	<b>Trial 1 (F)</b>	<b>Trial 2 (F)</b>	<b>Trial 3 (F)</b>	<b>Trial 4 (F)</b>	<b>Average</b>
7.5	74.4	75.6	75.6	75.9	75.375
6.5	75	76.5	76.5	76.4	76.1
5.5	75.1	77.4	77.8	77	76.825
4.5	76.9	80.2	78.2	79.4	78.675
3.5	77.5	82.4	79.9	81.8	80.4
2.5	84.3	85.9	82	82.6	83.7
1.5	96.2	95.1	88.4	84.6	91.075
0.5	116.2	104.9	136	105.2	115.575
0.25	164	280.4	364	546.4	338.7
0	1537	2204	1972	2407	2030

<b>T1 Ref</b>	73.1
<b>T2 Ref</b>	75.7
<b>T3 Ref</b>	74.2
<b>T4 Ref</b>	74.1

<b>Velocity 1.16</b>				
	<b>Trial 1 (C)</b>	<b>Trial 2 (C)</b>	<b>Trial 3 (C)</b>	<b>Trial 4 (C)</b>
<b>Temperature</b>	89.293	131.8223	77.8088	89.5224
<b>Average</b>	97.111625			

<b>Velocity 0.58</b>						
	<b>Trial 1 (C)</b>	<b>Trial 2 (C)</b>	<b>Trial 3 (C)</b>	<b>Trial 4 (C)</b>	<b>Trial 5 (C)</b>	<b>Trial 6 (C)</b>
<b>Temperature</b>	83.1355	86.22	156.1744	211.778	89.0451	177.2506
<b>Average</b>	133.9339333					

<b>Velocity 0.39</b>					
	<b>Trial 1 (C)</b>	<b>Trial 2 (C)</b>	<b>Trial 3 (C)</b>	<b>Trial 4 (C)</b>	<b>Trial 5 (C)</b>
<b>Temperature</b>	105.5268	118.6452	197.1795	101.4444	161.2553
<b>Average</b>	136.81024				

<b>Velocity 0.23</b>						
	<b>Trial 1 (C)</b>	<b>Trial 2 (C)</b>	<b>Trial 3 (C)</b>	<b>Trial 4 (C)</b>	<b>Trial 5 (C)</b>	<b>Trial 6 (C)</b>
<b>Temperature</b>	111.6519	126.4464	161.84	227.1561	185.4124	238.6052
<b>Average</b>	175.1853333					

<b>Velocity 0.14</b>					
	<b>Trial 1 (C)</b>	<b>Trial 2 (C)</b>	<b>Trial 3 (C)</b>	<b>Trial 4 (C)</b>	<b>Trial 5 (C)</b>
<b>Temperature</b>	274.917	235.9321	180.0869	337.0575	261.5983
<b>Average</b>	257.91836				

<b>Velocity .12</b>					
	<b>Trial 1 (C)</b>	<b>Trial 2 (C)</b>	<b>Trial 3 (C)</b>	<b>Trial 4 (C)</b>	<b>Trial 5 (C)</b>
<b>Temperature</b>	368.9834	324.3111	400.8341	371.2199	257.5306
<b>Average</b>	344.57582				

<b>Velocity .10</b>					
	<b>Trial 1 (C)</b>	<b>Trial 2 (C)</b>	<b>Trial 3 (C)</b>	<b>Trial 4 (C)</b>	<b>Trial 5 (C)</b>
<b>Temperature</b>	366.8099	395.6651	519.6282	377.2286	469.655
<b>Average</b>	425.79736				

<b>Velocity .08</b>					
	<b>Trial 1 (C)</b>	<b>Trial 2 (C)</b>	<b>Trial 3 (C)</b>	<b>Trial 4 (C)</b>	<b>Trial 5 (C)</b>
<b>Temperature</b>	426.6854	292.678	329.0377	294.5478	271.0064
<b>Average</b>	322.79106				

<b>Velocity .07</b>					
	<b>Trial 1 (C)</b>	<b>Trial 2 (C)</b>	<b>Trial 3 (C)</b>	<b>Trial 4 (C)</b>	<b>Trial 5 (C)</b>
<b>Temperature</b>	427.9195	477.0281	604.1109	409.6461	605.4193
<b>Average</b>	504.82478				

<b>Velocity .05</b>				
	<b>Trial 1 (C)</b>	<b>Trial 2 (C)</b>	<b>Trial 3 (C)</b>	<b>Trial 4 (C)</b>
<b>Temperature</b>	531.5618	652.6581	762.8342	707.103
<b>Average</b>	663.539275			

**Appendix M: Gas Equivalence Ratio 1 Corrected**

Preheat				
Distance (m)	Trial 1 (K)	Trial 2 (K)	Trial 3 (K)	Trial 4 (K)
0.1905	296.7056	297.3722	297.3722	297.5389
0.1651	297.0389	297.8722	297.8722	297.8167
0.1397	297.0944	298.3722	298.5944	298.1500
0.1143	298.0944	299.9278	298.8167	299.4833
0.0889	298.4278	301.1500	299.7611	300.8167
0.0635	302.2056	303.0944	300.9278	301.2611
0.0381	308.8167	308.2056	304.4833	302.3722
0.0127	319.9278	313.6500	330.9278	313.8167
0.00635	346.4833	411.1500	457.5944	558.9278
0	1109.2611	1479.8167	1350.9278	1592.5944

<b>T1 Ref</b>	295.9833333
<b>T2 Ref</b>	297.4277778
<b>T3 Ref</b>	296.5944444
<b>T4 Ref</b>	296.5388889
<b>Average</b>	296.6361111

Nusselt Number	
Velocity	Equivalence Ratio 1
1.156246528	16455.6566
0.578123264	4120.4681
0.385415509	1835.3390
0.231249306	7.9762
0.144530816	7.3453
0.115624653	6.8795
0.096353877	6.5176
0.082589038	6.0996
0.068014502	5.3806
0.046249861	5.3806

**Note: In order to determine corrected values, the noncorrected temperature was converted into Kelvin. Corrected Values are in degrees Celcius.**

<b>Velocity 1.16</b>				
	<b>Trial 1 (C)</b>	<b>Trial 2 (C)</b>	<b>Trial 3 (C)</b>	<b>Trial 4 (C)</b>
<b>Temperature</b>	89.293	131.8223	77.8088	89.5224
<b>Average</b>	97.111625	370.111625		
<b>Corrected</b>	97.112			

<b>Velocity 0.58</b>						
	<b>Trial 1 (C)</b>	<b>Trial 2 (C)</b>	<b>Trial 3 (C)</b>	<b>Trial 4 (C)</b>	<b>Trial 5 (C)</b>	<b>Trial 6 (C)</b>
<b>Temperature</b>	83.1355	86.22	156.1744	211.778	89.0451	177.2506
<b>Average</b>	133.9339333	406.9339333				
<b>Corrected</b>	133.9367517					

<b>Velocity 0.39</b>					
	<b>Trial 1 (C)</b>	<b>Trial 2 (C)</b>	<b>Trial 3 (C)</b>	<b>Trial 4 (C)</b>	<b>Trial 5 (C)</b>
<b>Temperature</b>	105.5268	118.6452	197.1795	101.4444	161.2553
<b>Average</b>	136.81024	409.81024			
<b>Corrected</b>	138.7760376				

<b>Velocity 0.23</b>						
	<b>Trial 1 (C)</b>	<b>Trial 2 (C)</b>	<b>Trial 3 (C)</b>	<b>Trial 4 (C)</b>	<b>Trial 5 (C)</b>	<b>Trial 6 (C)</b>
<b>Temperature</b>	111.6519	126.4464	161.84	227.1561	185.4124	238.6052
<b>Average</b>	448.1853333	721.1853333				
<b>Corrected</b>	459.1551239					

<b>Velocity 0.14</b>					
	<b>Trial 1 (C)</b>	<b>Trial 2 (C)</b>	<b>Trial 3 (C)</b>	<b>Trial 4 (C)</b>	<b>Trial 5 (C)</b>
<b>Temperature</b>	274.917	235.9321	180.0869	337.0575	261.5983
<b>Average</b>	257.91836	530.91836			
<b>Corrected</b>	262.3341838				

<b>Velocity .12</b>					
	<b>Trial 1 (C)</b>	<b>Trial 2 (C)</b>	<b>Trial 3 (C)</b>	<b>Trial 4 (C)</b>	<b>Trial 5 (C)</b>
<b>Temperature</b>	368.9834	324.3111	400.8341	371.2199	257.5306
<b>Average</b>	344.57582	617.57582			
<b>Corrected</b>	352.3601706				

<b>Velocity .10</b>					
	<b>Trial 1 (C)</b>	<b>Trial 2 (C)</b>	<b>Trial 3 (C)</b>	<b>Trial 4 (C)</b>	<b>Trial 5 (C)</b>
<b>Temperature</b>	366.8099	395.6651	519.6282	377.2286	469.655
<b>Average</b>	425.79736	698.79736			
<b>Corrected</b>	437.9619375				



<b>Velocity .08</b>					
	<b>Trial 1 (C)</b>	<b>Trial 2 (C)</b>	<b>Trial 3 (C)</b>	<b>Trial 4 (C)</b>	<b>Trial 5 (C)</b>
<b>Temperature</b>	426.6854	292.678	329.0377	294.5478	271.0064
<b>Average</b>	322.79106	595.79106			
<b>Corrected</b>	330.6055557				

<b>Velocity .07</b>					
	<b>Trial 1 (C)</b>	<b>Trial 2 (C)</b>	<b>Trial 3 (C)</b>	<b>Trial 4 (C)</b>	<b>Trial 5 (C)</b>
<b>Temperature</b>	427.9195	477.0281	604.1109	409.6461	605.4193
<b>Average</b>	504.82478	777.82478			
<b>Corrected</b>	525.3832659				

<b>Velocity .05</b>				
	<b>Trial 1 (C)</b>	<b>Trial 2 (C)</b>	<b>Trial 3 (C)</b>	<b>Trial 4 (C)</b>
<b>Temperature</b>	531.5618	652.6581	762.8342	707.103
<b>Average</b>	663.539275	936.539275		
<b>Corrected</b>	699.8316849			

**Appendix N: Gas Equivalence Ratio Raw Data**

<b>Preheat</b>				
<b>Distance (in)</b>	<b>Trial 1</b>	<b>Trial 2</b>	<b>Trial 3</b>	<b>Trial 4</b>
7.5	76.1	76.7	78	78
6.5	76.3	77.9	81.1	78.5
5.5	76.9	78.2	85	80
4.5	80	82.4	85.3	84.1
3.5	83.6	82.7	84.4	87.5
2.5	85.1	84.4	88.6	88.9
1.5	89.4	87.9	92.3	94.8
0.5	123.7	122.1	130.5	134.8
0.25	238.4	295.5	395.3	266.9
0	1712	2065	1575	2272

<b>T1 Ref</b>	75.4
<b>T2 Ref</b>	74.9
<b>T3 Ref</b>	75.2
<b>T4 Ref</b>	73.5

<b>Velocity 1.16</b>					
	<b>Trial 1 (C)</b>	<b>Trial 2 (C)</b>	<b>Trial 3 (C)</b>	<b>Trial 4 (C)</b>	<b>Trial 5 (C)</b>
<b>Temperature</b>	74.1418	126.0754	91.9328	80.8427	70.8434
<b>Average</b>	88.76722				

<b>Velocity 0.58</b>				
	<b>Trial 1 (C)</b>	<b>Trial 2 (C)</b>	<b>Trial 3 (C)</b>	<b>Trial 4 (C)</b>
<b>Temperature</b>	109.8441	160.9346	141.5056	160.3677
<b>Average</b>	143.163			

<b>Velocity 0.39</b>					
	<b>Trial 1 (C)</b>	<b>Trial 2 (C)</b>	<b>Trial 3 (C)</b>	<b>Trial 4 (C)</b>	<b>Trial 5 (C)</b>
<b>Temperature</b>	225.8654	180.2033	135.7582	178.9462	109.5802
<b>Average</b>	166.07066				

<b>Velocity 0.23</b>					
	<b>Trial 1 (C)</b>	<b>Trial 2 (C)</b>	<b>Trial 3 (C)</b>	<b>Trial 4 (C)</b>	<b>Trial 5 (C)</b>
<b>Temperature</b>	354.2454	339.5421	281.227	272.2078	202.1564
<b>Average</b>	289.87574				

<b>Velocity 0.14</b>					
	<b>Trial 1 (C)</b>	<b>Trial 2 (C)</b>	<b>Trial 3 (C)</b>	<b>Trial 4 (C)</b>	<b>Trial 5 (C)</b>
<b>Temperature</b>	337.2942	527.7859	277.0661	292.6877	350.0011
<b>Average</b>	356.967				

<b>Velocity .12</b>					
	<b>Trial 1 (C)</b>	<b>Trial 2 (C)</b>	<b>Trial 3 (C)</b>	<b>Trial 4 (C)</b>	<b>Trial 5 (C)</b>
<b>Temperature</b>	452.2964	345.359	503.8556	406.873	
<b>Average</b>	427.096				

<b>Velocity .10</b>					
	<b>Trial 1 (C)</b>	<b>Trial 2 (C)</b>	<b>Trial 3 (C)</b>	<b>Trial 4 (C)</b>	<b>Trial 5 (C)</b>
<b>Temperature</b>	476.8344	375.3535	456.9462	513.4056	
<b>Average</b>	455.634925				

<b>Velocity .08</b>					
	<b>Trial 1 (C)</b>	<b>Trial 2 (C)</b>	<b>Trial 3 (C)</b>	<b>Trial 4 (C)</b>	<b>Trial 5 (C)</b>
<b>Temperature</b>	411.5598	299.0515	468.3534	471.2856	
<b>Average</b>	412.562575				

<b>Velocity .07</b>						
	<b>Trial 1 (C)</b>	<b>Trial 2 (C)</b>	<b>Trial 3 (C)</b>	<b>Trial 4 (C)</b>	<b>Trial 5 (C)</b>	<b>Trial 6 (C)</b>
<b>Temperature</b>	639.9214	429.1428	290.8762	647.4007	765.5896	717.9448
<b>Average</b>	581.8125833					

<b>Velocity .05</b>				
	<b>Trial 1 (C)</b>	<b>Trial 2 (C)</b>	<b>Trial 3 (C)</b>	<b>Trial 4 (C)</b>
<b>Temperature</b>	691.2527	622.7269	735.5086	531.7418
<b>Average</b>	645.3075			

**Appendix N: Gas Equivalence Ratio 2 Corrected**

<b>T1 Ref (F)</b>	75.4	<b>Average (F)</b>	<b>Average (K)</b>
<b>T2 Ref (F)</b>	74.9	74.75	296.75
<b>T3 Ref (F)</b>	75.2		
<b>T4 Ref (F)</b>	73.5		

<b>Preheat</b>				
<b>Distance (in)</b>	<b>Trial 1 (F)</b>	<b>Trial 2 (F)</b>	<b>Trial 3 (F)</b>	<b>Trial 4 (F)</b>
7.5	76.1	76.7	78	78
6.5	76.3	77.9	81.1	78.5
5.5	76.9	78.2	85	80
4.5	80	82.4	85.3	84.1
3.5	83.6	82.7	84.4	87.5
2.5	85.1	84.4	88.6	88.9
1.5	89.4	87.9	92.3	94.8
0.5	123.7	122.1	130.5	134.8
0.25	238.4	295.5	395.3	266.9
0	1712	2065	1575	2272

**Note: In order to determine corrected values, the noncorrected temperature was converted into Kelvin. Corrected Values are in degrees Celcius.**

<b>Velocity 1.16</b>					
	<b>Trial 1 (C)</b>	<b>Trial 2 (C)</b>	<b>Trial 3 (C)</b>	<b>Trial 4 (C)</b>	<b>Trial 5 (C)</b>
<b>Temperature</b>	74.1418	126.0754	91.9328	80.8427	70.8434
<b>Average</b>	88.76722	361.76722			
<b>Corrected</b>	88.76726046				

<b>Velocity 0.58</b>				
	<b>Trial 1 (C)</b>	<b>Trial 2 (C)</b>	<b>Trial 3 (C)</b>	<b>Trial 4 (C)</b>
<b>Temperature</b>	109.8441	160.9346	141.5056	160.3677
<b>Average</b>	143.163	416.163		
<b>Corrected</b>	143.1632936			

<b>Velocity 0.39</b>					
	<b>Trial 1 (C)</b>	<b>Trial 2 (C)</b>	<b>Trial 3 (C)</b>	<b>Trial 4 (C)</b>	<b>Trial 5 (C)</b>
<b>Temperature</b>	225.8654	180.2033	135.7582	178.9462	109.5802
<b>Average</b>	166.07066	439.07066			
<b>Corrected</b>	166.07135				

<b>Velocity 0.23</b>					
	<b>Trial 1 (C)</b>	<b>Trial 2 (C)</b>	<b>Trial 3 (C)</b>	<b>Trial 4 (C)</b>	<b>Trial 5 (C)</b>
<b>Temperature</b>	354.2454	339.5421	281.227	272.2078	202.1564
<b>Average</b>	289.87574	562.87574			
<b>Corrected</b>	289.8812544				

<b>Velocity 0.14</b>					
	<b>Trial 1 (C)</b>	<b>Trial 2 (C)</b>	<b>Trial 3 (C)</b>	<b>Trial 4 (C)</b>	<b>Trial 5 (C)</b>
<b>Temperature</b>	337.2942	527.7859	277.0661	292.6877	350.0011
<b>Average</b>	356.967	629.967			
<b>Corrected</b>	356.9750206				

<b>Velocity .12</b>					
	<b>Trial 1 (C)</b>	<b>Trial 2 (C)</b>	<b>Trial 3 (C)</b>	<b>Trial 4 (C)</b>	<b>Trial 5 (C)</b>
<b>Temperature</b>	452.2964	345.359	503.8556	406.873	
<b>Average</b>	427.096	700.096			
<b>Corrected</b>	427.1072358				

<b>Velocity .10</b>					
	<b>Trial 1 (C)</b>	<b>Trial 2 (C)</b>	<b>Trial 3 (C)</b>	<b>Trial 4 (C)</b>	<b>Trial 5 (C)</b>
<b>Temperature</b>	476.8344	375.3535	456.9462	513.4056	
<b>Average</b>	455.634925	728.634925			
<b>Corrected</b>	455.6476801				

<b>Velocity .08</b>					
	<b>Trial 1 (C)</b>	<b>Trial 2 (C)</b>	<b>Trial 3 (C)</b>	<b>Trial 4 (C)</b>	<b>Trial 5 (C)</b>
<b>Temperature</b>	411.5598	299.0515	468.3534	471.2856	
<b>Average</b>	412.562575	685.562575			
<b>Corrected</b>	412.573133				

<b>Velocity .07</b>						
	<b>Trial 1 (C)</b>	<b>Trial 2 (C)</b>	<b>Trial 3 (C)</b>	<b>Trial 4 (C)</b>	<b>Trial 5 (C)</b>	<b>Trial 6 (C)</b>
<b>Temperature</b>	639.9214	429.1428	290.8762	647.4007	765.5896	717.9448
<b>Average</b>	581.8125833	854.8125833				
<b>Corrected</b>	581.8335255					

<b>Velocity .05</b>				
	<b>Trial 1 (C)</b>	<b>Trial 2 (C)</b>	<b>Trial 3 (C)</b>	<b>Trial 4 (C)</b>
<b>Temperature</b>	691.2527	622.7269	735.5086	531.7418
<b>Average</b>	645.3075	918.3075		
<b>Corrected</b>	645.3336423			

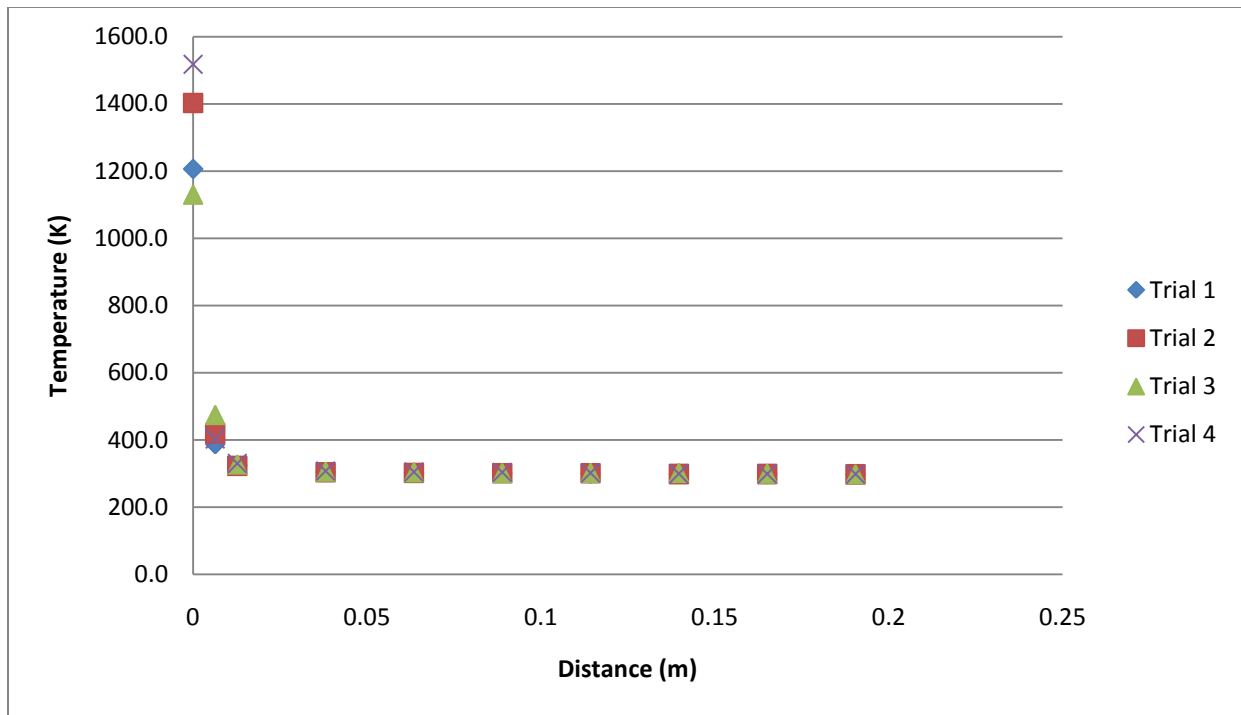


Figure 18: Gas Flame Preheat Temperature vs. Distance for an Equivalence Ratio of 0.78

**Appendix O: Gas Equivalence Ratio 3 Raw Data**

<b>Preheat</b>					
<b>Distance (in)</b>	<b>Temp (F)</b>	<b>Trial 1</b>	<b>Trial 2</b>	<b>Trial 3</b>	<b>Trial 4</b>
7.5		75.7	75.9	78.7	77
6.5		76.2	76.8	78.4	79.4
5.5		76.4	77.1	78.7	82.5
4.5		77.1	78.4	82.2	83.5
3.5		78.6	80.8	83.4	89.8
2.5		79.5	87.3	89.7	90.1
1.5		87.3	96.7	97.4	98.1
0.5		114.3	139.8	119.9	117.4
0.25		268.1	447.4	473.4	506
0		1893	1592	1938	1955

<b>T1 Ref</b>	74.5
<b>T2 Ref</b>	73.7
<b>T3 Ref</b>	73.6
<b>T4 Ref</b>	73

<b>Velocity 1.16</b>				
	<b>Trial 1 (C)</b>	<b>Trial 2 (C)</b>	<b>Trial 3 (C)</b>	<b>Trial 4 (C)</b>
<b>Temperature</b>	115.6188	194.5582	109.4268	172.3177
<b>Average</b>	147.980375			

<b>Velocity 0.58</b>					
	<b>Trial 1 (C)</b>	<b>Trial 2 (C)</b>	<b>Trial 3 (C)</b>	<b>Trial 4 (C)</b>	<b>Trial 5 (C)</b>
<b>Temperature</b>	153.4754	372.2686	305.855	175.3369	208.2137
<b>Average</b>	243.02992				

<b>Velocity 0.39</b>						
	<b>Trial 1 (C)</b>	<b>Trial 2 (C)</b>	<b>Trial 3 (C)</b>	<b>Trial 4 (C)</b>	<b>Trial 5 (C)</b>	<b>Trial 6 (C)</b>
<b>Temperature</b>	377.6546	214.3068	179.6004	446.5616	182.5224	186.2343
<b>Average</b>	264.4800167					

<b>Velocity 0.23</b>					
	<b>Trial 1 (C)</b>	<b>Trial 2 (C)</b>	<b>Trial 3 (C)</b>	<b>Trial 4 (C)</b>	<b>Trial 5 (C)</b>
<b>Temperature</b>	469.7988	602.6169	317.6236	220.6987	325.9737
<b>Average</b>	387.34234				

<b>Velocity 0.14</b>					
	<b>Trial 1 (C)</b>	<b>Trial 2 (C)</b>	<b>Trial 3 (C)</b>	<b>Trial 4 (C)</b>	<b>Trial 5 (C)</b>
<b>Temperature</b>	617.6885	508.7253	363.4465	717.5717	375.3236
<b>Average</b>	516.55112				

<b>Velocity .12</b>					
	<b>Trial 1 (C)</b>	<b>Trial 2 (C)</b>	<b>Trial 3 (C)</b>	<b>Trial 4 (C)</b>	<b>Trial 5 (C)</b>
<b>Temperature</b>	630.3573	634.2554	400.1013	419.6298	591.3393
<b>Average</b>	535.13662				

<b>Velocity .10</b>					
	<b>Trial 1 (C)</b>	<b>Trial 2 (C)</b>	<b>Trial 3 (C)</b>	<b>Trial 4 (C)</b>	<b>Trial 5 (C)</b>
<b>Temperature</b>	589.1876	912.6359	613.2715	864.5503	512.9379
<b>Average</b>	698.51664				

<b>Velocity .08</b>					
	<b>Trial 1 (C)</b>	<b>Trial 2 (C)</b>	<b>Trial 3 (C)</b>	<b>Trial 4 (C)</b>	<b>Trial 5 (C)</b>
<b>Temperature</b>	916.1208	906.6438	942.8818	891.7473	711.0264
<b>Average</b>	873.68402				

<b>Velocity .07</b>					
	<b>Trial 1 (C)</b>	<b>Trial 2 (C)</b>	<b>Trial 3 (C)</b>	<b>Trial 4 (C)</b>	
<b>Temperature</b>	820.1246	844.4611	717.9846	810.0293	
<b>Average</b>	798.1499				

<b>Velocity .05</b>				
	<b>Trial 1 (C)</b>	<b>Trial 2 (C)</b>	<b>Trial 3 (C)</b>	<b>Trial 4 (C)</b>
<b>Temperature</b>	869.052	855.5818	973.6863	979.0073
<b>Average</b>	919.33185			



**Appendix P: Gas Equivalence Ratio 3 Corrected**

<b>T1 Ref (F)</b>	75.4	<b>Average (F)</b>	<b>Average (K)</b>
<b>T2 Ref (F)</b>	74.9	74.75	296.75
<b>T3 Ref (F)</b>	75.2		
<b>T4 Ref (F)</b>	73.5		

<b>Preheat</b>				
<b>Distance (in)</b>	<b>Trial 1 (F)</b>	<b>Trial 2 (F)</b>	<b>Trial 3 (F)</b>	<b>Trial 4 (F)</b>
7.5	76.1	76.7	78	78
6.5	76.3	77.9	81.1	78.5
5.5	76.9	78.2	85	80
4.5	80	82.4	85.3	84.1
3.5	83.6	82.7	84.4	87.5
2.5	85.1	84.4	88.6	88.9
1.5	89.4	87.9	92.3	94.8
0.5	123.7	122.1	130.5	134.8
0.25	238.4	295.5	395.3	266.9
0	1712	2065	1575	2272

**Note: In order to determine corrected values, the noncorrected temperature was converted into Kelvin. Corrected Values are in degrees Celcius.**

<b>Velocity 1.16</b>				
	<b>Trial 1 (C)</b>	<b>Trial 2 (C)</b>	<b>Trial 3 (C)</b>	<b>Trial 4 (C)</b>
<b>Temperature</b>	115.6188	194.5582	109.4268	172.3177
<b>Average</b>	147.980375	420.980375		
<b>Corrected</b>	147.9803754			

<b>Velocity 0.58</b>				
	<b>Trial 1 (C)</b>	<b>Trial 2 (C)</b>	<b>Trial 3 (C)</b>	<b>Trial 4 (C)</b>
<b>Temperature</b>	109.8441	160.9346	141.5056	160.3677
<b>Average</b>	143.163	416.163		
<b>Corrected</b>	143.1630014			

<b>Velocity 0.39</b>					
	<b>Trial 1 (C)</b>	<b>Trial 2 (C)</b>	<b>Trial 3 (C)</b>	<b>Trial 4 (C)</b>	<b>Trial 5 (C)</b>
<b>Temperature</b>	225.8654	180.2033	135.7582	178.9462	109.5802
<b>Average</b>	166.07066	439.07066			
<b>Corrected</b>	166.0706639				

<b>Velocity 0.23</b>					
	<b>Trial 1 (C)</b>	<b>Trial 2 (C)</b>	<b>Trial 3 (C)</b>	<b>Trial 4 (C)</b>	<b>Trial 5 (C)</b>
<b>Temperature</b>	354.2454	339.5421	281.227	272.2078	202.1564
<b>Average</b>	289.87574	562.87574			
<b>Corrected</b>	289.8770367				

<b>Velocity 0.14</b>					
	<b>Trial 1 (C)</b>	<b>Trial 2 (C)</b>	<b>Trial 3 (C)</b>	<b>Trial 4 (C)</b>	<b>Trial 5 (C)</b>
<b>Temperature</b>	337.2942	527.7859	277.0661	292.6877	350.0011
<b>Average</b>	356.967	629.967			
<b>Corrected</b>	356.9692345				

<b>Velocity .12</b>					
	<b>Trial 1 (C)</b>	<b>Trial 2 (C)</b>	<b>Trial 3 (C)</b>	<b>Trial 4 (C)</b>	<b>Trial 5 (C)</b>
<b>Temperature</b>	452.2964	345.359	503.8556	406.873	
<b>Average</b>	427.096	700.096			
<b>Corrected</b>	427.0993818				

<b>Velocity .10</b>					
	<b>Trial 1 (C)</b>	<b>Trial 2 (C)</b>	<b>Trial 3 (C)</b>	<b>Trial 4 (C)</b>	<b>Trial 5 (C)</b>
<b>Temperature</b>	476.8344	375.3535	456.9462	513.4056	
<b>Average</b>	455.634925	728.634925			
<b>Corrected</b>	455.6390074				

<b>Velocity .08</b>					
	<b>Trial 1 (C)</b>	<b>Trial 2 (C)</b>	<b>Trial 3 (C)</b>	<b>Trial 4 (C)</b>	<b>Trial 5 (C)</b>
<b>Temperature</b>	411.5598	299.0515	468.3534	471.2856	
<b>Average</b>	412.562575	685.562575			
<b>Corrected</b>	412.5661299				

<b>Velocity .07</b>						
	<b>Trial 1 (C)</b>	<b>Trial 2 (C)</b>	<b>Trial 3 (C)</b>	<b>Trial 4 (C)</b>	<b>Trial 5 (C)</b>	<b>Trial 6 (C)</b>
<b>Temperature</b>	639.9214	429.1428	290.8762	647.4007	765.5896	717.9448
<b>Average</b>	581.8125833	854.8125833				
<b>Corrected</b>	581.8200867					

<b>Velocity .05</b>				
	<b>Trial 1 (C)</b>	<b>Trial 2 (C)</b>	<b>Trial 3 (C)</b>	<b>Trial 4 (C)</b>
<b>Temperature</b>	691.2527	622.7269	735.5086	531.7418
<b>Average</b>	645.3075	918.3075		
<b>Corrected</b>	645.3180344			

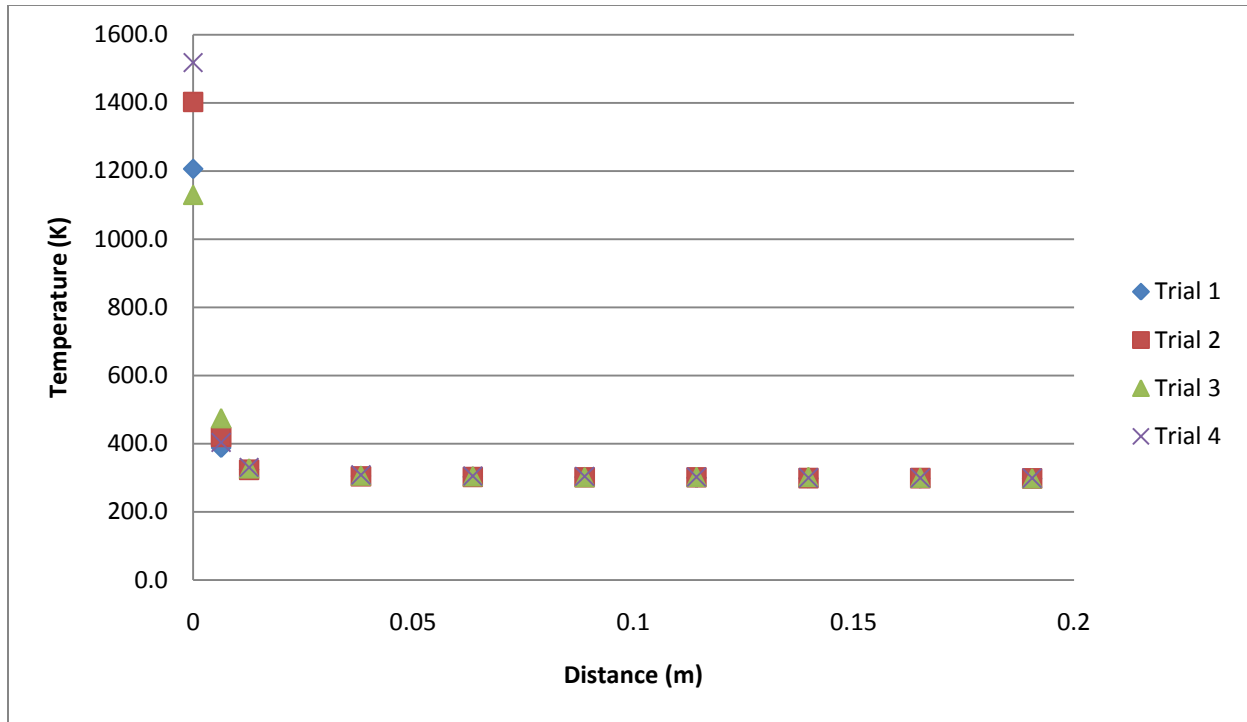


Figure 19: Gas Flame Preheat Temperature vs. Distance for an Equivalence Ratio of 1.16

**Appendix Q: Gas Equivalence Ratio 4 Raw Data**

<b>Preheat</b>				
<b>Distance (in)</b>	<b>Trial 1 (F)</b>	<b>Trial 2 (F)</b>	<b>Trial 3 (F)</b>	<b>Trial 4 (F)</b>
7.5	76.2	76	77.8	76.3
6.5	76.8	77.9	77.2	78.3
5.5	79.4	79.6	82.4	81.8
4.5	80	80.4	84.8	81.9
3.5	82.2	82.7	85.1	82.2
2.5	85.7	83.8	89.9	90.1
1.5	89.1	97.3	92.6	92.3
0.5	135.1	142.4	132.5	131.7
0.25	411.1	508.2	365.8	430.4
0	1859	2170	1915	2330

<b>T1 Ref</b>	72.7
<b>T2 Ref</b>	73.1
<b>T3 Ref</b>	74.6
<b>T4 Ref</b>	73.1

<b>Velocity 1.16</b>					
	<b>Trial 1 (C)</b>	<b>Trial 2 (C)</b>	<b>Trial 3 (C)</b>	<b>Trial 4 (C)</b>	<b>Trial 5 (C)</b>
<b>Temperature</b>	154.7224	161.2837	99.5701	221.0319	143.3587
<b>Average</b>	155.99336				

<b>Velocity 0.58</b>								
	<b>Trial 1 (C)</b>	<b>Trial 2 (C)</b>	<b>Trial 3 (C)</b>	<b>Trial 4 (C)</b>	<b>Trial 5 (C)</b>	<b>Trial 6 (C)</b>	<b>Trial 7 (C)</b>	<b>Trial 8 (C)</b>
<b>Temperature</b>	142.7534	167.6104	170.2245	238.4158	212.7574	330.8936	273.5927	193.1388
<b>Average</b>	216.173325							

<b>Velocity 0.39</b>					
	<b>Trial 1 (C)</b>	<b>Trial 2 (C)</b>	<b>Trial 3 (C)</b>	<b>Trial 4 (C)</b>	<b>Trial 5 (C)</b>
<b>Temperature</b>	456.2279	169.0951	222.5705	564.0765	181.8651
<b>Average</b>	318.76702				

<b>Velocity 0.23</b>					
	<b>Trial 1 (C)</b>	<b>Trial 2 (C)</b>	<b>Trial 3 (C)</b>	<b>Trial 4 (C)</b>	<b>Trial 5 (C)</b>
<b>Temperature</b>	538.2484	250.0449	608.6398	312.05	580.6959
<b>Average</b>	457.9358				

<b>Velocity 0.14</b>					
	<b>Trial 1 (C)</b>	<b>Trial 2 (C)</b>	<b>Trial 3 (C)</b>	<b>Trial 4 (C)</b>	<b>Trial 5 (C)</b>
<b>Temperature</b>	650.578	740.1022	700.2193	579.202	880.681
<b>Average</b>	710.1565				

<b>Velocity .12</b>						
	<b>Trial 1 (C)</b>	<b>Trial 2 (C)</b>	<b>Trial 3 (C)</b>	<b>Trial 4 (C)</b>	<b>Trial 5 (C)</b>	<b>Trial 6 (C)</b>
<b>Temperature</b>	947.7246	905.6156	419.3993	495.8752	942.9258	553.9351
<b>Average</b>	710.9126					

<b>Velocity .10</b>						
	<b>Trial 1 (C)</b>	<b>Trial 2 (C)</b>	<b>Trial 3 (C)</b>	<b>Trial 4 (C)</b>	<b>Trial 5 (C)</b>	<b>Trial 6 (C)</b>
<b>Temperature</b>	740.9251	836.0758	971.0942	410.7505	608.8619	813.184
<b>Average</b>	730.1485833					

<b>Velocity .08</b>						
	<b>Trial 1 (C)</b>	<b>Trial 2 (C)</b>	<b>Trial 3 (C)</b>	<b>Trial 4 (C)</b>	<b>Trial 5 (C)</b>	<b>Trial 6 (C)</b>
<b>Temperature</b>	971.1318	507.2685	884.6068	957.7878	830.0422	823.3823
<b>Average</b>	829.0365667					

<b>Velocity .07</b>						
	<b>Trial 1 (C)</b>	<b>Trial 2 (C)</b>	<b>Trial 3 (C)</b>	<b>Trial 4 (C)</b>	<b>Trial 5 (C)</b>	<b>Trial 6 (C)</b>
<b>Temperature</b>	971.1318	507.2685	884.6068	957.7878	830.0422	823.3823
<b>Average</b>	829.0365667					

<b>Velocity .05</b>						
	<b>Trial 1 (C)</b>	<b>Trial 2 (C)</b>	<b>Trial 3 (C)</b>	<b>Trial 4 (C)</b>	<b>Trial 5 (C)</b>	<b>Trial 6 (C)</b>
<b>Temperature</b>	928.9998	970.4924	987.5613	979.6001	906.3074	977.4604
<b>Average</b>	958.4035667					

**Appendix R: Gas Equivalence Ratio 4 Corrected**

<b>T1 Ref (F)</b>	72.7	<b>Average (F)</b>	<b>Average (K)</b>
<b>T2 Ref (F)</b>	73.1	73.375	295.9861111
<b>T3 Ref (F)</b>	74.6		
<b>T4 Ref (F)</b>	73.1		

<b>Preheat</b>				
<b>Distance (in)</b>	<b>Trial 1 (F)</b>	<b>Trial 2 (F)</b>	<b>Trial 3 (F)</b>	<b>Trial 4 (F)</b>
7.5	76.2	76	77.8	76.3
6.5	76.8	77.9	77.2	78.3
5.5	79.4	79.6	82.4	81.8
4.5	80	80.4	84.8	81.9
3.5	82.2	82.7	85.1	82.2
2.5	85.7	83.8	89.9	90.1
1.5	89.1	97.3	92.6	92.3
0.5	135.1	142.4	132.5	131.7
0.25	411.1	508.2	365.8	430.4
0	1859	2170	1915	2330

**Note: In order to determine corrected values, the noncorrected temperature was converted into Kelvin. Corrected Values are in degrees Celcius.**

<b>Velocity 1.16</b>					
	<b>Trial 1 (C)</b>	<b>Trial 2 (C)</b>	<b>Trial 3 (C)</b>	<b>Trial 4 (C)</b>	<b>Trial 5 (C)</b>
<b>Temperature</b>	154.7224	161.2837	99.5701	221.0319	143.3587
<b>Average</b>	155.99336	428.99336			
<b>Corrected</b>	155.9933601				

<b>Velocity 0.58</b>								
	<b>Trial 1 (C)</b>	<b>Trial 2 (C)</b>	<b>Trial 3 (C)</b>	<b>Trial 4 (C)</b>	<b>Trial 5 (C)</b>	<b>Trial 6 (C)</b>	<b>Trial 7 (C)</b>	<b>Trial 8 (C)</b>
<b>Temperature</b>	142.7534	167.6104	170.2245	238.4158	212.7574	330.8936	273.5927	193.1388
<b>Average</b>	216.173325	489.173325						
<b>Corrected</b>	216.173326							

<b>Velocity 0.39</b>					
	<b>Trial 1 (C)</b>	<b>Trial 2 (C)</b>	<b>Trial 3 (C)</b>	<b>Trial 4 (C)</b>	<b>Trial 5 (C)</b>
<b>Temperature</b>	456.2279	169.0951	222.5705	564.0765	181.8651
<b>Average</b>	318.76702	591.76702			
<b>Corrected</b>	318.7670242				

<b>Velocity 0.23</b>					
	<b>Trial 1 (C)</b>	<b>Trial 2 (C)</b>	<b>Trial 3 (C)</b>	<b>Trial 4 (C)</b>	<b>Trial 5 (C)</b>
<b>Temperature</b>	538.2484	250.0449	608.6398	312.05	580.6959
<b>Average</b>	457.9358	730.9358			
<b>Corrected</b>	457.9358229				

<b>Velocity 0.14</b>					
	<b>Trial 1 (C)</b>	<b>Trial 2 (C)</b>	<b>Trial 3 (C)</b>	<b>Trial 4 (C)</b>	<b>Trial 5 (C)</b>
<b>Temperature</b>	650.578	740.1022	700.2193	579.202	880.681
<b>Average</b>	710.1565	983.1565			
<b>Corrected</b>	710.1638883				

<b>Velocity .12</b>						
	<b>Trial 1 (C)</b>	<b>Trial 2 (C)</b>	<b>Trial 3 (C)</b>	<b>Trial 4 (C)</b>	<b>Trial 5 (C)</b>	<b>Trial 6 (C)</b>
<b>Temperature</b>	947.7246	905.6156	419.3993	495.8752	942.9258	553.9351
<b>Average</b>	710.9126	983.9126				
<b>Corrected</b>	710.9206643					

<b>Velocity .10</b>						
	<b>Trial 1 (C)</b>	<b>Trial 2 (C)</b>	<b>Trial 3 (C)</b>	<b>Trial 4 (C)</b>	<b>Trial 5 (C)</b>	<b>Trial 6 (C)</b>
<b>Temperature</b>	740.9251	836.0758	971.0942	410.7505	608.8619	813.184
<b>Average</b>	730.1485833	1003.148583				
<b>Corrected</b>	730.1577363					

<b>Velocity .08</b>						
	<b>Trial 1 (C)</b>	<b>Trial 2 (C)</b>	<b>Trial 3 (C)</b>	<b>Trial 4 (C)</b>	<b>Trial 5 (C)</b>	<b>Trial 6 (C)</b>
<b>Temperature</b>	971.1318	507.2685	884.6068	957.7878	830.0422	823.3823
<b>Average</b>	829.0365667	1102.036567				
<b>Corrected</b>	829.0494342					

<b>Velocity .07</b>						
	<b>Trial 1 (C)</b>	<b>Trial 2 (C)</b>	<b>Trial 3 (C)</b>	<b>Trial 4 (C)</b>	<b>Trial 5 (C)</b>	<b>Trial 6 (C)</b>
<b>Temperature</b>	971.1318	507.2685	884.6068	957.7878	830.0422	823.3823
<b>Average</b>	829.0365667	1102.036567				
<b>Corrected</b>	829.0503539					

<b>Velocity .05</b>						
	<b>Trial 1 (C)</b>	<b>Trial 2 (C)</b>	<b>Trial 3 (C)</b>	<b>Trial 4 (C)</b>	<b>Trial 5 (C)</b>	<b>Trial 6 (C)</b>
<b>Temperature</b>	928.9998	970.4924	987.5613	979.6001	906.3074	977.4604
<b>Average</b>	958.4035667	1231.403567				
<b>Corrected</b>	958.4255399					

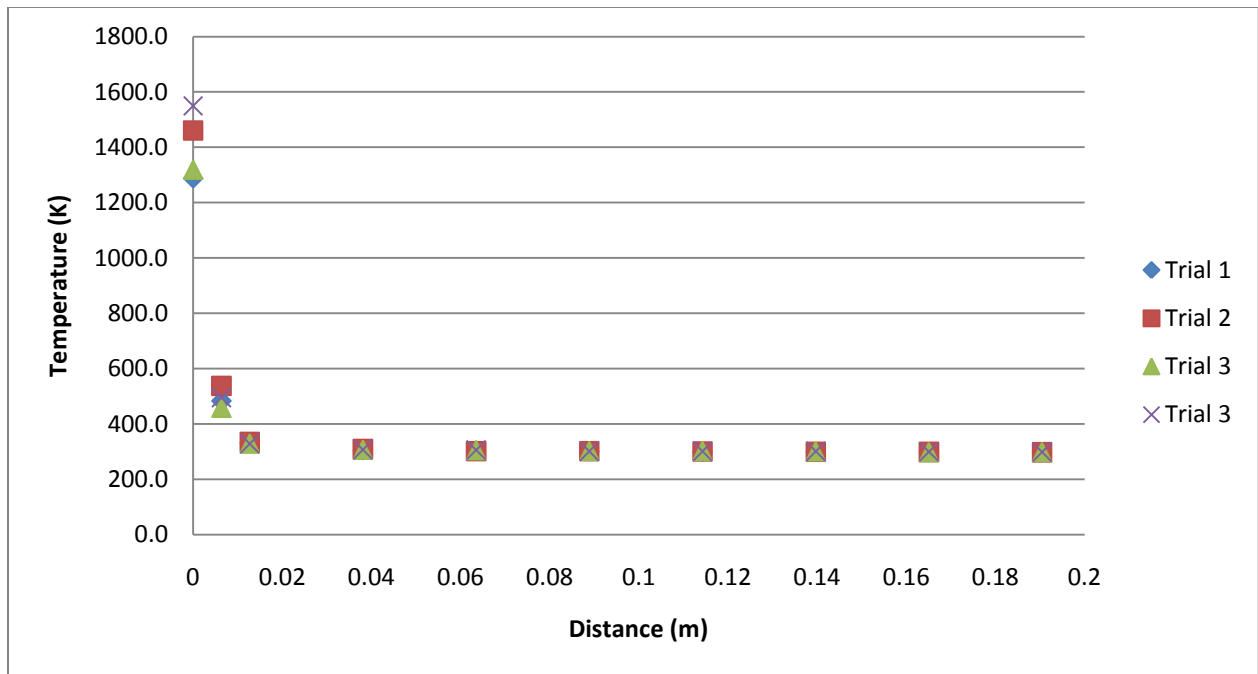


Figure 20: Gas Flame Preheat Temperature vs. Distance for an Equivalence Ratio of 1.37



**Appendix S: Dust Equivalence Ratio Raw Data**

Preheat distance (in)	Preheat Temp ( C)
7.5	67.6
6.5	67.8
5.5	68.8
4.5	70
3.5	71.9
2.5	75.5
1.5	99.8
0.5	142.5
0.25	425.7
0	1530

Deviation of +5%	Deviation of -5%
70.98	64.22
71.19	64.41
72.24	65.36
73.5	66.5
75.495	68.305
79.275	71.725
104.79	94.81
149.625	135.375
446.985	404.415
1606.5	1453.5

Velocity 1.16						
	Trial 1 (C)	Trial 2 (C)	Trial 3 (C)	Trial 4 (C)	Trial 5 (C)	Trial 6 (C)
Temperature	159.6029	170.8966	244.8909	221.0319	181.716	221.2449
Average	199.8972	472.8972				

Velocity 0.58								
	Trial 1 (C)	Trial 2 (C)	Trial 3 (C)	Trial 4 (C)	Trial 5 (C)	Trial 6 (C)	Trial 7 (C)	Trial 8 (C)
Temperature	244.7436	183.7422	161.6866	238.4158	212.7574	330.8936	273.5927	193.1388
Average	229.8713375	502.8713375						

Velocity 0.39					
	Trial 1 (C)	Trial 2 (C)	Trial 3 (C)	Trial 4 (C)	Trial 5 (C)
Temperature					
Average					

<b>Velocity 0.23</b>			
	<b>Trial 1 (C)</b>	<b>Trial 2 (C)</b>	<b>Trial 3 (C)</b>
<b>Temperature</b>	136.2765	121.8841	144.0749
<b>Average</b>	134.0785	407.0785	

<b>Velocity 0.14</b>					
	<b>Trial 1 (C)</b>	<b>Trial 2 (C)</b>	<b>Trial 3 (C)</b>	<b>Trial 4 (C)</b>	<b>Trial 5 (C)</b>
<b>Temperature</b>	135.2144	115.9002			
<b>Average</b>	125.5573	398.5573			

<b>Velocity .12</b>				
	<b>Trial 1 (C)</b>	<b>Trial 2 (C)</b>	<b>Trial 3 (C)</b>	<b>Trial 4 (C)</b>
<b>Temperature</b>	156.1703	136.6421	192.1371	133.2187
<b>Average</b>	154.54205	427.54205		

<b>Velocity .10</b>						
	<b>Trial 1 (C)</b>	<b>Trial 2 (C)</b>	<b>Trial 3 (C)</b>	<b>Trial 4 (C)</b>	<b>Trial 5 (C)</b>	<b>Trial 6 (C)</b>
<b>Temperature</b>	152.4717	109.5027	155.5834	197.7088	230.2757	233.7256
<b>Average</b>	179.8779833	452.8779833				

<b>Velocity .08</b>					
	<b>Trial 1 (C)</b>	<b>Trial 2 (C)</b>	<b>Trial 3 (C)</b>	<b>Trial 4 (C)</b>	<b>Trial 5 (C)</b>
<b>Temperature</b>	98.6833	117.6167	341.7621	371.1839	101.9452
<b>Average</b>	206.23824	479.23824			

<b>Velocity .07</b>				
	<b>Trial 1 (C)</b>	<b>Trial 2 (C)</b>	<b>Trial 3 (C)</b>	<b>Trial 4 (C)</b>
<b>Temperature</b>	487.2053	182.1489	419.5509	299.8883
<b>Average</b>	347.19835	620.19835		

<b>Velocity .05</b>					
	<b>Trial 1 (C)</b>	<b>Trial 2 (C)</b>	<b>Trial 3 (C)</b>	<b>Trial 4 (C)</b>	<b>Trial 5 (C)</b>
<b>Temperature</b>	377.9173	277.1209	314.6842	448.5871	274.0321
<b>Average</b>	338.46832	611.46832			

**Appendix T: Dust Equivalence Ratio Corrected**

Ref Temp (F)	Ref Temp (K)
72.8	295.666667

Preheat	
Distance (in)	Trial 1 (F)
7.5	67.6
6.5	67.8
5.5	68.8
4.5	70
3.5	71.9
2.5	75.5
1.5	99.8
0.5	142.5
0.25	425.7
0	1530

**Note: In order to determine corrected values, the noncorrected temperature was converted into Kelvin. Corrected Values are in degrees Celcius.**

Velocity .12				
	Trial 1 (C)	Trial 2 (C)	Trial 3 (C)	Trial 4 (C)
Temperature	156.1703	136.6421	192.1371	133.2187
Average	154.54205	427.54205		
Corrected	156.2250535			

Velocity .10						
	Trial 1 (C)	Trial 2 (C)	Trial 3 (C)	Trial 4 (C)	Trial 5 (C)	Trial 6 (C)
Temperature	152.4717	109.5027	155.5834	197.7088	230.2757	233.7256
Average	179.8779833	452.8779833				
Corrected	182.1526815					

Velocity .08					
	Trial 1 (C)	Trial 2 (C)	Trial 3 (C)	Trial 4 (C)	Trial 5 (C)
Temperature	98.6833	117.6167	341.7621	371.1839	101.9452
Average	206.23824	479.23824			
Corrected	209.2213952				

<b>Velocity .07</b>				
	<b>Trial 1 (C)</b>	<b>Trial 2 (C)</b>	<b>Trial 3 (C)</b>	<b>Trial 4 (C)</b>
<b>Temperature</b>	487.2053	182.1489	419.5509	299.8883
<b>Average</b>	347.19835	620.19835		
<b>Corrected</b>	354.8941735			

<b>Velocity .05</b>					
	<b>Trial 1 (C)</b>	<b>Trial 2 (C)</b>	<b>Trial 3 (C)</b>	<b>Trial 4 (C)</b>	<b>Trial 5 (C)</b>
<b>Temperature</b>	377.9173	277.1209	314.6842	448.5871	274.0321
<b>Average</b>	338.46832	611.46832			
<b>Corrected</b>	346.8803326				

## Appendix U: Theoretical Critical Distance

D	R	h (m)	View Factor	Heat Flux
0.00635	0.008980256	1	5.1339E-05	45.64642648
0.006684211	0.009452901	0.95	5.68849E-05	50.57746413
0.007055556	0.009978062	0.9	6.33806E-05	56.35290231
0.007470588	0.010565007	0.85	7.10559E-05	63.17714046
0.0079375	0.01122532	0.8	8.02147E-05	71.32038465
0.008466667	0.011973675	0.75	9.12654E-05	81.14580966
0.009071429	0.012828937	0.7	0.000104768	93.15076023
0.009769231	0.013815779	0.65	0.000121503	108.0309409
0.010583333	0.014967094	0.6	0.000142595	126.783512
0.011545455	0.016327738	0.55	0.000169695	150.8785749
0.0127	0.017960512	0.5	0.000205323	182.5562634
0.014111111	0.019956125	0.45	0.000253472	225.3667372
0.015875	0.02245064	0.4	0.000320778	285.2096689
0.018142857	0.025657875	0.35	0.000418932	372.4804509
0.021166667	0.029934187	0.3	0.000570123	506.9069821
0.0254	0.035921024	0.25	0.000820761	729.7543718
0.03175	0.044901281	0.2	0.00128182	1139.690279
0.042333333	0.059868374	0.15	0.002276415	2024.003395
0.0635	0.089802561	0.1	0.005106723	4540.483428

D	R	h (m)	View Factor	Heat Flux
0.03175	0.044901	0.2	0.00128182	1139.690279
0.033421	0.047265	0.19	0.001420093	1262.631644
0.035278	0.04989	0.18	0.001581996	1406.582231
0.037353	0.052825	0.17	0.001773231	1576.613303
0.039688	0.056127	0.16	0.002001333	1779.42277
0.042333	0.059868	0.15	0.002276415	2024.003395

D	R	h (m)	View Factor	Heat Flux
0.037353	0.052825	0.17	0.001773231	1576.613303
0.037798	0.053454	0.168	0.001815622	1614.303377
0.038253	0.054098	0.166	0.00185955	1653.360396
0.03872	0.054758	0.164	0.00190509	1693.851226
0.038957	0.055094	0.163	0.00192849	1714.656338
0.039688	0.056127	0.16	0.002001333	1779.42277

Time to Pain	s
0.12 m/s	6.966666667
0.10 m/s	8.36
0.08 m/s	10.45
0.07 m/s	11.94285714
0.05 m/s	16.72

<b>Pre-heat time:</b>	<b>s</b>
0.12 m/s	1.3625
0.10 m/s	1.635
0.08 m/s	2.04375
0.07 m/s	2.335714286
0.05 m/s	3.27